

Review

Thermodynamics of Thermoelectric Phenomena and Applications

Christophe Goupil^{1,*}, Wolfgang Seifert², Knud Zabrocki³, Eckhard Müller³ and G. Jeffrey Snyder⁴

¹ Laboratoire CRISMAT, UMR 6508, Caen 14050, France

² Institute of Physics, University Halle-Wittenberg, D-06099 Halle (Saale), Germany;

E-Mail: wolfgang.seifert@physik.uni-halle.de

³ Institute of Materials Research, German Aerospace Center (DLR), D-51170 Köln, Germany;

E-Mails: knud.zabrocki@dlr.de (K.Z.); eckhard.mueller@dlr.de (E.M.)

⁴ California Institute of Technology, Pasadena, CA 91125, USA; E-Mail: jsnyder@caltech.edu

* Author to whom correspondence should be addressed; E-Mail: christophe.goupil@ensicaen.fr; Fax: +33-2-31-45-26-35.

Received: 2 July 2011; in revised form: 15 July 2011 / Accepted: 29 July 2011 /

Published: 15 August 2011

Abstract: Fifty years ago, the optimization of thermoelectric devices was analyzed by considering the relation between optimal performances and local entropy production. Entropy is produced by the irreversible processes in thermoelectric devices. If these processes could be eliminated, entropy production would be reduced to zero, and the limiting Carnot efficiency or coefficient of performance would be obtained. In the present review, we start with some fundamental thermodynamic considerations relevant for thermoelectrics. Based on a historical overview, we reconsider the interrelation between optimal performances and local entropy production by using the compatibility approach together with the thermodynamic arguments. Using the relative current density and the thermoelectric potential, we show that minimum entropy production can be obtained when the thermoelectric potential is a specific, optimal value.

Keywords: thermoelectricity; optimum device design; entropy production; compatibility approach; thermoelectric potential

1. Introduction

1.1. Historical Notes

Thermoelectric (TE) phenomena were discovered at the beginning of the 19th century first by Thomas J. Seebeck, who observed the deviation of a compass needle when keeping the two junctions of different metals at different temperatures [1–3]. This effect [4] illustrates the coupling of two thermodynamic potentials, the electrochemical potential and the temperature. Shortly thereafter, in 1834, Jean C. A. Peltier discovered the inverse effect that under isothermal conditions an electrical current can cause a temperature difference at the junction [5]. Later on, in 1851, William Thomson (known later as Lord Kelvin), brought the theory of thermoelectrics into harmony with the two laws of thermodynamics. By using thermodynamic arguments he unified the Seebeck and Peltier effects into one single expression giving decisive arguments in favor of a complete and compact description of all these phenomena [6]. With this theoretical analysis of the relationship between both effects he was able to show that a third effect has to exist. This third effect bearing his name is the absorption or generation of heat along a conductor carrying current under a thermal gradient.

At the beginning of the 20th century both the theory and the application had been observed again [7,8]. Particularly worth mentioning are two theoretical papers by E. Altenkirch (who was certainly inspired by older investigations, among others Lord Rayleigh [9]) about the efficiency of a thermopile [10], which has been used to generate electrical energy for various special purposes, and a separate work about the effectiveness of thermoelectric cooling [11]. Comparing the results with the efficiency of the Carnot cycle, he characterizes the thermopile as a “rather imperfect thermodynamic engine”. Altenkirch gave first evidence that a good TE material should have a large Seebeck coefficient α , a high electrical conductivity σ (low specific electrical resistance) to minimize Joule heating and a low thermal conductivity [12] κ to retain heat at the junctions and maintain a large temperature gradients.

For metals and metallic alloys, the Seebeck coefficient (and thus the figure of merit) is rather low. It took until the 1930's when Maria Telkes made a thorough study of the Pb S-Zn Sb couple to develop a better material [13–17].

Almost at the same time Lars Onsager proposed a theoretical description of linear non-equilibrium thermodynamic processes where the coupled thermodynamic forces and fluxes are described in a very general form. In two major articles, the fundamentals of thermodynamics of dissipative transport were developed in a consistent way [18,19]. A summary can be found in a later work of Onsager [20]. Note that Onsager expressed initial thoughts on the dissipation function and the principle of least dissipation of energy, see [18,19].

The thermodynamic theory of TE phenomena in isotropic media was first worked out by H. B. Callen [21,22] and is presented in more detail in de Groot's monograph [23]. Usually denoted as Onsager–de Groot–Callen theory, it might be called a “first approximation” theory of TE transport giving a coherent thermodynamic description of TE processes on a phenomenological level. Domenicali's fundamental article [24] summarizes the principles of steady-state thermodynamics applied to a TE system out of thermostatic equilibrium. He pointed out that a complete description of the state includes the determination of the “electrochemical potential” from the overall electronic and crystalline structure of all phases constituting the TE system.

The usage of semiconductors as thermoelectric materials was responsible for a revival of thermoelectrics in the late 1950's [25]. This is directly connected with the investigations of Goldsmid [26] and Ioffe [27] who considered both thermodynamics and solid state approaches. They extended the previous developments to the microscopic area opening the door for material engineering and practical applications. Ioffe introduced the figure of merit as a primary parameter which gathers the different transport coefficients, leading to an efficient classification of the various TE materials. His publications can be seen as outstanding works of literature in the field of thermoelectrics even today, see, e.g., [25,27–29].

The introduction of the irreversible entropy production in the form of an equality is a very old problem mentioned by Lord Kelvin himself. Tolman and Fine [30] were probably the first to point out that the entropy production of a TE process can be considered as a measure of the total irreversibilities. Before that, Bridgman discussed the relation between thermodynamics and thermoelectrics in several articles [31–34]. At the beginning of the 1930's Sommerfeld and Frank gave an review about the statistical theory of thermoelectric phenomena in metals, but without considering entropy production [35]. Their calculation is based on Darrow's report [36]. In 1952 Haase [37] presented a review about the thermodynamic-phenomenological theory of irreversible processes containing thoughts about thermoelectrics, too. During the 1950's and 1960's, a very active period of thermoelectrics, there were a lot of works dedicated to the topic of this review. For a small selection we draw the reader's attention to [24,38–55]. Another work should be particularly emphasized: Sherman, Heikes and Ure stated in [47] that the conditions which maximize the TEG's efficiency are precisely the conditions which minimize the irreversibility process, allowing a closer approach to the Carnot cycle where entropy production is zero. This concept had been deepened by Clingman [49,50] for TEG and TEC.

After a very active period of investigations the interest in thermoelectricity collapsed under the weight of inflated hopes, because there had been no significant advances in efficiency after the mid-1960's. As breakthroughs in the field decelerated, basic research in thermoelectrics lay stagnant for 30 years after that, meanwhile some materials and commercial uses were still developed. In between this period some few works on the topic had been made [56–64].

New ideas and materials in the mid-1990's brought thermoelectrics back into the scope of research. The search for green technologies, e.g., converting waste heat generated by car engines into usable power, pushes scientists to pick up "old" effects with new classes of materials with higher thermoelectric efficiency to have practical applications using the advantages of thermoelectric power generation [65–67]. An overview of different applications is given by Riffat *et al.* in [68]. For the thermodynamic theory of thermoelectric materials and devices in the period from the 1990s to today, the reader may consult, e.g., [69–94] and references therein.

The content of this review paper includes seven sections. In the next subsection, we derive the thermodynamics of thermoelectricity from the classical thermodynamics of cyclical systems. The second section is devoted to the Onsager description of non-equilibrium thermodynamics of coupled transport processes. In the third section the consequences of the Onsager theory are derived, leading to the expressions of heat and entropy production. The fourth section summarizes TE applications, and the fifth section is devoted to the presentation of the general conductance matrix. Using these last two

sections, the concepts of relative current and thermoelectric potential are exposed in the sixth section. In the last section, we close this article with comments on optimum device design and functionally graded materials.

1.2. The Thermoelectric Engine

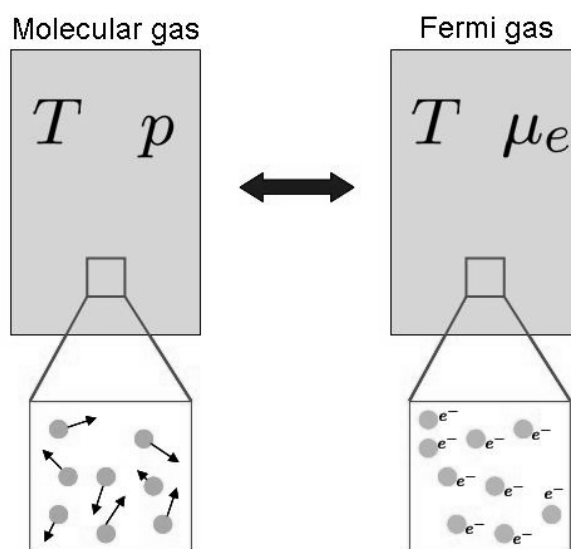
We propose to consider the analogies between a classical steam engine and a thermoelectric material [95]. The analogy is that in both systems, the entropy is transported by a fluid, which is here a gas of electrons, also called the “Fermi gas”. At first this Fermi gas can be considered to be a perfect gas, with no interactions between particles [96]. Then the equivalent “partial pressure” p of the fluid in the system is the electrochemical potential μ_e

$$\mu_e = \mu_c + e \mathcal{V}$$

where μ_c is the chemical potential [97], e the particle’s charge [98] and \mathcal{V} the electrical potential. Then the “gas” equivalences for the steam and thermoelectric engines are:

In a first approach, as usually done for traditional steam engines, only the fluid is considered and the walls of the enclosure containing this fluid are not taken into account. These walls contribution to the global efficiency are not considered, neither the boiling walls of the steam engine, nor the lattice vibrations (phonons) of the thermoelectric material. Then we have a similar picture of the two systems (see Figure 1), not only for the fluid (steam or electronic gas), but also for the thermal leak (boiling walls or lattice vibrations) as symbolically shown in Figure 2.

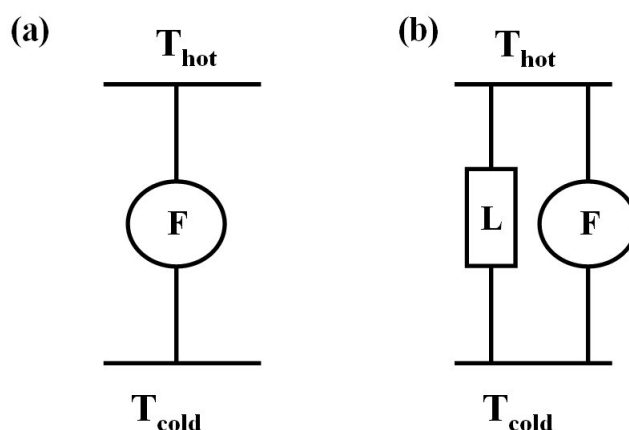
Figure 1. Comparison between steam and thermoelectric engine.



As we observe, the efficiency of the engine is reduced by the presence of a heat leak. As a consequence, materials with very low lattice thermal conductivity are highly required for thermoelectric applications. Let us consider now a sample of thermoelectric material where one end is maintained at the temperature T_h and the other at temperature T_c with $T_h > T_c$. If we consider the Fermi gas inside the sample then we get from elementary statistical arguments a large velocity and small gas density at the hot end and a small velocity and large gas density at the cold end. It should be noticed that since

heat flows from the hot to the cold end, the system cannot be considered under equilibrium conditions although the averaged carrier flux is zero: particles are going from cold to hot and hot to cold side, but the two opposing fluxes are equal since the cell is closed. We also see that the gradient of carrier density is directly driven by the temperature gradient. Since the carriers are charged particles, we get an electrochemical difference, commonly called voltage difference, which is induced by the application of a temperature difference. This illustrates the coupling of the electrochemical potential gradient and the temperature. Next, since the averaged carrier flux is zero, but heat is transported at the same time, we get the same values of particle fluxes from hot to cold and from cold to hot. From this observation we can conclude that heat and carrier fluxes are coupled. While very simple, this description contains the main contributions to thermoelectric processes. In the ideal, reversible case without entropy production this would be a Carnot cycle containing two “isothermal” processes, respectively at hot and cold side, and two “adiabatic” processes from hot to cold side and from cold to hot side.

Figure 2. Dithermal thermodynamic engine: The cycling working fluid is marked as F and the thermal leak is marked as L. (a) ideal model neglecting the engine walls; (b): realistic model including the thermal leaks.



Actually, since the thermoelectric process is not ideal, we can then estimate the principle sources of entropy of the working system that are the non-isothermal heat transfers and the non-adiabatic travel of the carriers from cold to hot sources and hot to cold. This entropy production in the non-adiabatic branches are due to the collisions between carriers and the interactions with the crystal lattice of the material.

In Section 2.5 we will focus on the entropy transported by the carriers of the Fermi gas, which will be defined as the “entropy per carrier” which is a fundamental parameter of the thermoelectric process. As previously mentioned, it should be stressed again that the present description does not explicitly mention the atoms of the crystal lattice that provide parasitic thermal conduction due to phonons or other thermal conduction mechanisms. This is due to the Onsager description which follows the so called linear response theory where the linear response Fourier’s law is used. Fourier’s law is valid for thermal conduction due to phonons as well as electrons and is therefore included in the phenomenological description. If these two processes are independent then it is common to describe

the thermal conductivity in absence of carrier transport as $\kappa_J = \kappa_e + \kappa_{\text{Lat}}$ where κ_e is the electronic contribution and κ_{Lat} is the lattice contribution.

2. Forces & Fluxes

2.1. Irreversible Thermodynamics and the Onsager–de Groot–Callen Model

Since a thermodynamic system is a statistical assembly of subsystems, the equilibrium of a thermodynamic system is not a static picture of the system but a configuration where the fluctuations of the intensive parameters (T, p, \dots) are very small compared to their average values. This may be called a fluctuation-average condition (FAC). It is obvious that this definition only applies for systems being not too small since the ratio of fluctuations to the average value diverges for very small numbers of particles. The link with the microscopic scale is then direct since every intensive parameter refers to a specific distribution spectrum. For example, the equilibrium temperature refers to a time invariant spectrum of the distribution of the particle velocities. As a consequence this implies very short microscopic relaxation times in comparison with the macroscopic system relaxation time. In other words, the system is considered to be ergodic. It should be mentioned that this definition is also correct in the case of out-of-equilibrium systems, since it can be defined as a sum of subsystems that may fulfill the FAC at local state, leading to the conclusion that a local equilibrium can be defined. As a consequence, the definition of intensive parameters can be extended, at local state, to macroscopic non-equilibrium systems. Then the system exhibits a mapping of spatial variation of these intensive parameters, which may vary over the time until their variation is very slow compared to the microscopic relaxation times. In this article we will further simplify the problem and assume that all non-equilibrium processes are steady-state processes which means that the previous mapping is constant over the time, or may vary very slowly compared to the microscopic relaxation time. From a system evolution point of view, this is nothing more than a definition of a quasi-static transformation. Readers interested in a more detailed presentation of steady-state irreversible processes like electric current flow and heat conduction in semiconductor, metals and other solid state systems may find interesting developments in some specific literature: we refer for a brief review of the basics of irreversible thermodynamics, e.g., to [23,99], and further to the book by N. Tschoegl [100] providing a good introduction for steady-state thermodynamics.

For small perturbations (near equilibrium problems) one can assume linear coupling between TD forces and fluxes. The driving forces which may bring the system as close as possible back to equilibrium are derived from the intensive parameters of the system. According to a linear response approach they are conjugated to fluxes, like Ohm's law and Fourier's law.

In a thermoelectric system, the thermal and electrical processes are coupled. Since the thermoelectric process described above is not under equilibrium conditions, the thermodynamic intensive parameters, such as μ_e and T , need to be properly defined using non-equilibrium thermodynamics. It should be noticed here that the underlying mechanisms for these forces to bring the system back to equilibrium are not straightforward, nor general, since there is no general minimal principle for such a process. Nevertheless, under non-equilibrium conditions the system's evolution is assumed to be driven by a minimal production of entropy due to the coupling of the potentials. In other words, any given fluctuating potential undergoes a restoring force due to the presence of the others [101]. As a consequence we get

a stationary picture, where all the thermodynamic potentials are clearly defined, though the system itself produces dissipation. As previously said, this is nothing more than a definition of a quasi-static process since the system is considered to head back to local equilibrium at each time. This leads to the very important result that the classical quasi-static relation $dS = dQ_{qs}/T$ between the heat and the entropy variation can be extended to finite time response thermodynamics in the following flux form

$$\mathbf{J}_S = \frac{\mathbf{J}_Q}{T} \quad (1)$$

where \mathbf{J}_S and \mathbf{J}_Q are the entropy flux and heat flux density. Then we get a continuous thermodynamic description, where the thermodynamic equilibrium, where all average fluxes equal zero, just becomes one possible thermodynamic state for the system.

The domain of validity of the Onsager description is then limited to non-equilibrium stationary states near equilibrium which has been described by Prigogine's theorem of minimum entropy production [102,103]. It states that, in a time-dependent system, the rate of entropy production will monotonically decrease until the system gets as close to equilibrium as possible, also taking into account the externally applied constraints (temperature and electrochemical potential differences). These latter, called *working conditions*, can be fulfilled or not, leading to an overall minimal entropy production that can be very far from its optimal value. This point will be reconsidered in Section 6 by using the thermoelectric potential, which is a part of the free energy of the system under non-equilibrium conditions. Finally, one can notice that the Onsager description is nothing more than a generalization of the Fluctuation-Dissipation theorem of coupled processes, where it is assumed that at a stable steady state the dissipation function is minimum, or more precisely that the linear (and stationary) response of a system and the noisy response of this system are linked by the same fundamental mechanisms [104–107].

2.2. Forces and Fluxes

The Onsager force-flux derivation is obtained from the laws of conservation of energy and matter. If we consider the complete energy flux, then the first law of thermodynamics gives the expression of the total energy flux \mathbf{J}_E , heat flux \mathbf{J}_Q and particles flux \mathbf{J}_N ,

$$\mathbf{J}_E = \mathbf{J}_Q + \mu_e \mathbf{J}_N \quad (2)$$

Each of these fluxes are conjugated to their thermodynamic potential gradients, which, as general forces, derive from the thermodynamic potentials. The question of the correct expression of these potentials is out of the scope of the present article, but it can be shown the correct potentials for energy and particles are respectively $\frac{1}{T}$ and $\frac{\mu_e}{T}$ [104]. Using the Nabla or Del operator ∇ , the corresponding forces can be expressed as their gradients

$$\mathbf{F}_N = \nabla \left(-\frac{\mu_e}{T} \right), \quad \mathbf{F}_E = \nabla \left(\frac{1}{T} \right) \quad (3)$$

and the linear coupling between forces and fluxes can simply be derived by a linear set of coupled equations with kinetic coefficient matrix $[L]$,

$$\begin{bmatrix} \mathbf{J}_N \\ \mathbf{J}_E \end{bmatrix} = \begin{bmatrix} L_{NN} & L_{NE} \\ L_{EN} & L_{EE} \end{bmatrix} \begin{bmatrix} \nabla \left(-\frac{\mu_e}{T} \right) \\ \nabla \left(\frac{1}{T} \right) \end{bmatrix}$$

where $L_{NE} = L_{EN}$. The symmetry of the off-diagonal term is fundamental in the Onsager description since it is equivalent to a minimal entropy production of the system under non-equilibrium conditions [101]. A first experimental verification of the Onsager reciprocal relations had been given by Miller for different materials [46]. As we already pointed out, the minimal entropy production is not a general property of non-equilibrium processes. However, under steady-state conditions, a fluctuating thermodynamic potential will undergo a restoring force due to the presence of another potential. This mechanism has to be symmetric, and so do the off-diagonal terms of the kinetic matrix $[L]$ [108]. From a microscopic point of view this equality also implies the time reversal symmetry of the processes [109]. By extension processes at micro scale should be “micro reversible”. Since the irreversibility is a statistical consequence of the number of particles inside the considered system, then, at a microscopic scale, “irreversible thermodynamics” simply becomes a “reversible dynamics”.

2.3. Energy Flux and Heat Flux

In order to treat properly heat and carrier fluxes it is more convenient to rewrite the second equation of the above matrix formulation for $\mathbf{J}_Q = \mathbf{J}_E - \mu_e \mathbf{J}_N$. Doing this it is advantageous to change slightly the first force in order to let appear explicitly μ_e and not only $\nabla(-\frac{\mu_e}{T})$. Using the expansion

$$\nabla\left(-\frac{\mu_e}{T}\right) = -\frac{1}{T} \nabla\mu_e - \mu_e \nabla\left(\frac{1}{T}\right)$$

a straightforward calculation gives

$$\begin{bmatrix} \mathbf{J}_N \\ \mathbf{J}_Q \end{bmatrix} = \begin{bmatrix} L_{11} & L_{12} \\ L_{21} & L_{22} \end{bmatrix} \begin{bmatrix} -\frac{1}{T} \nabla\mu_e \\ \nabla\left(\frac{1}{T}\right) \end{bmatrix} \tag{4}$$

with $L_{12} = L_{21}$ and the kinetic coefficients become

$$L_{11} = L_{NN}, \quad L_{12} = L_{NE} - \mu_e L_{NN}, \quad L_{22} = L_{EE} - \mu_e(L_{EN} + L_{NE}) + \mu_e^2 L_{NN} \tag{5}$$

Since the electric field derives from the electrochemical potential, see Section 1.2, we also get

$$\mathbf{E} = -\frac{\nabla\mu_e}{e} = -\frac{\nabla\mu_c}{e} - \nabla\mathcal{V} \tag{6}$$

2.4. Thermoelectric Coefficients

Depending on the thermodynamic working conditions, the thermoelectric coefficients can be derived from the two expressions of particle and heat flux density.

2.4.1. Decoupled Processes

Using Expression (4) under isothermal conditions, we get the electrical current density in the form

$$\mathbf{J} = \frac{-e L_{11}}{T} \nabla\mu_e \tag{7}$$

where $\mathbf{J} = e\mathbf{J}_N$. This is an expression of Ohm’s law. The isothermal electrical conductivity is

$$\sigma_T = \frac{e^2}{T} L_{11} \tag{8}$$

Alternatively, if we consider the heat flux density in the absence of any particle transport, or under zero electrical current then we get

$$\mathbf{J} = \mathbf{0} = -L_{11} \left(\frac{\nabla \mu_e}{T} \right) + L_{12} \nabla \left(\frac{1}{T} \right) \quad (9)$$

and the heat flux density becomes

$$\mathbf{J}_{Q_J} = \frac{1}{T^2} \left(\frac{L_{21}L_{12} - L_{11}L_{22}}{L_{11}} \right) \nabla T \quad (10)$$

which is Fourier's law, where the thermal conductivity under zero electrical current (open circuit) is

$$\kappa_J = \frac{1}{T^2} \left(\frac{L_{11}L_{22} - L_{21}L_{12}}{L_{11}} \right) \quad (11)$$

Finally, we can also consider the thermal conductivity under zero electrochemical gradient (closed circuit), then we get

$$\mathbf{J}_{Q_E} = \frac{L_{22}}{T^2} \nabla T \quad \text{with} \quad \kappa_E = \frac{L_{22}}{T^2} \quad (12)$$

2.4.2. Coupled Processes

Let us now consider the TE coupling in more detail. In the absence of any particle transport, the basic expression is already known since it is given by Equation (9). If we now define the Seebeck coefficient as the ratio between the electrochemical gradient and the temperature gradient, then the Seebeck coefficient expression is given by

$$-\frac{1}{e} \nabla \mu_e \equiv \alpha \nabla T = \mathbf{E}|_{J=0} \quad (13)$$

For the electric field relation see also Section 2.6. Using Equation (9) we finally find for Seebeck

$$\alpha = \frac{1}{eT} \frac{L_{12}}{L_{11}} \quad (14)$$

If we consider now an isothermal configuration, we can derive the expression of the coupling term between current density and heat flux which is nothing more than the Peltier coefficient

$$\mathbf{J} = e L_{11} \left(-\frac{1}{T} \nabla \mu_e \right), \quad \mathbf{J}_Q = L_{21} \left(-\frac{1}{T} \nabla \mu_e \right) \quad (15)$$

we get

$$\mathbf{J}_Q = \frac{1}{e} \frac{L_{12}}{L_{11}} \mathbf{J} \quad (16)$$

and the Peltier coefficient Π is given by

$$\mathbf{J}_Q = \Pi \mathbf{J}, \quad \Pi = \frac{1}{e} \frac{L_{12}}{L_{11}} \quad (17)$$

As one can see, we have the equality

$$\Pi = \alpha T$$

The close connection between Peltier and Seebeck effects is illustrated by this compact expression. In a later paragraph we will show that a similar connection can be derived for the Thomson effect. From a fundamental point of view this shows that all of these effects are in fact different expressions of the same quantity, called the "entropy per carrier", defined by Callen [110,111]. It will be considered first, followed by the definitions of the transport parameters.

2.5. The Entropy per Carrier

Using the classical approach of the thermodynamic cycle we can consider a carrier traveling through the different steps of the Carnot cycle. Focusing on the two adiabatic branches of the thermodynamic cycle, it appears that a certain amount of entropy is driven from the hot side to the cold side, but also from the cold side to the hot side. In this convective process, the carrier acts as if it was carrying some entropy. Let us derive this by considering the entropy flux density. From the heat flux density expression we can write

$$\mathbf{J}_S = \frac{1}{T} \left[L_{21} \left(-\frac{1}{T} \nabla \mu_e \right) + L_{22} \nabla \left(\frac{1}{T} \right) \right] \tag{18}$$

According to Ohm’s law, see Equation (7), it can be simplified into

$$\mathbf{J}_S = \frac{L_{21}}{T e L_{11}} \mathbf{J} + \frac{1}{T} L_{22} \nabla \left(\frac{1}{T} \right) \tag{19}$$

We see here that the entropy flux contains two terms, one from electrochemical origin and the other from thermal origin. The first term shows that a fraction of the entropy is transported by the flux of carriers. Then the entropy transported per carrier (or per particle) is given by

$$S_N = \frac{L_{21}}{T L_{11}} \tag{20}$$

As one can see, the Seebeck coefficient is directly proportional to S_N since we have

$$S_N = e \alpha \tag{21}$$

It is important to note that the entropy per particle is a fundamental parameter from which all the thermoelectric effects derive. Nevertheless, the reader should take care not to attribute a specific entropy to each carrier. Since thermodynamics never considers an isolated particle but only a large number of particles, the definition of the entropy per particle refers to an averaged property of the Fermion gas, as a statistical definition. This is also valid for the $S_N = e \alpha$ expression where the Seebeck effect cannot be reduced to the direct summation of the individual contribution of the carriers. As an illustration one can see that S_N is a function of the electrical conductivity through the term L_{11} . The conductive models, like the Drude model, cannot be derived at the scale of a carrier with the attribution of a specific electrical conductivity to each carrier.

2.6. Kinetic Coefficients and Transport Parameters

Using the entropy per carrier S_N defined in the previous Section 2.5 we can get now a complete correspondence between the kinetic coefficients and the transport parameters. We have

$$\frac{L_{11}}{\frac{T}{e^2} \sigma_T} \quad \frac{L_{12} = L_{21}}{\frac{T^2}{e^2} \sigma_T S_N} \quad \frac{L_{22}}{\frac{T^3}{e^2} \sigma_T S_N^2 + T^2 \kappa_J}$$

and the Onsager expressions become

$$\mathbf{J} = -\sigma_T \left(\frac{\nabla \mu_e}{e} \right) + \frac{\sigma_T S_N T^2}{e^2} \nabla \left(\frac{1}{T} \right) \tag{22}$$

$$\mathbf{J}_Q = -T \sigma_T S_N \left(\frac{\nabla \mu_e}{e} \right) + \left(\frac{T^3}{e^2} \sigma_T S_N^2 + T^2 \kappa_J \right) \nabla \left(\frac{1}{T} \right) \tag{23}$$

Finally, we distinguish between the thermal conductivity under zero electrochemical gradient and under zero particle transport,

$$\kappa_E = \frac{L_{22}}{T^2}, \quad \kappa_J = \frac{1}{T^2} \left(\frac{L_{11}L_{22} - L_{21}L_{12}}{L_{11}} \right) \tag{24}$$

leading to the equality

$$\kappa_E = T\alpha^2\sigma_T + \kappa_J \tag{25}$$

Setting Equation (22) into Equation (23) and using the local expansions $\nabla(\frac{1}{T}) = -\frac{1}{T^2}\nabla T$ and $\mathbf{E} = -\frac{\nabla\mu}{e}$, the “classical” expressions

$$\mathbf{J} = \sigma_T\mathbf{E} - \sigma_T\alpha\nabla T \quad \text{and} \quad \mathbf{J}_Q = \alpha T\mathbf{J} - \kappa_J\nabla T$$

are reproduced, see also [95]. Then, it follows that $\mathbf{E} = \alpha\nabla T + \rho\mathbf{J}$ with electrical resistivity $\rho = 1/\sigma_T$.

2.7. The Dimensionless Figure of Merit zT

We have seen from the kinetic matrix $[L]$ that the off-diagonal terms represent the coupling between the heat flux and the electrical flux. The question now is how to optimize a given material to get an efficient heat pump driven by an input electric current or an efficient thermoelectric generator driven by a supplied heat flow. The procedure can be derived for both applications, but we propose here to consider a thermogenerator application.

Let us first look at the optimization of the fluxes. Since a thermoelectric material is an energy conversion device, the more heat flows into the material, the more electrical power may be produced. In order to achieve this we expect a large thermal conductivity for the material. Unfortunately this will also lead to a very small temperature difference and consequently a small electrical output voltage and power. This configuration can be called the short-circuit configuration since the fluxes are maximized and the potential differences minimized.

Now we consider the coupled processes from the potential point of view. In order to get a larger voltage the material should exhibit a large temperature difference. Then the thermal conductivity of the material should be as small as possible, leading to a very small heat flux and consequently, again, a small electrical power output. This configuration can be called the open-circuit configuration since the potential differences are maximized and the fluxes are minimized.

It is worth noting that both short-circuit and open-circuit configurations lead to a non-satisfactory solution. Moreover they are in contradiction since the thermal conductivity is expected to be maximal in the short-circuit configuration and minimal in the open-circuit one! This contradiction can be resolved if we consider the expression of the thermal conductivities previously given by

$$\kappa_E = T\alpha^2\sigma_T + \kappa_J \tag{26}$$

Since it is established under zero current, the κ_J corresponds to the open-circuit configuration while κ_E corresponds to the short-circuit configuration. From the previous derivations, see Equation (25), we expect $\frac{\kappa_E}{\kappa_J}$ to be maximal in order to get the maximal output electrical power. Then we can write

$$\frac{\kappa_E}{\kappa_J} = \left[\frac{\alpha^2\sigma_T T}{\kappa_J} + 1 \right] \tag{27}$$

with the figure of merit zT defined by

$$zT = \frac{\alpha^2 \sigma_T}{\kappa_J} T \tag{28}$$

In 1961 C. Zener defined a similar ratio of the thermal conductivities as a “thermoelectric coupling factor”, see [112]:

$$f = \frac{\kappa_E - \kappa_J}{\kappa_J} \tag{29}$$

which coincides with the figure of merit, see Equation (28). Another definition of the coupling factor is the following ratio

$$f = \frac{\sigma_T - \sigma_S}{\sigma_S} \tag{30}$$

where σ_S and σ_T are the electrical conductivities under conditions of zero entropy flux and zero temperature gradient. As one can notice from Equation (27), the zT term should be maximal in order to get an optimal material. The thermoelectric properties of the material are summarized in the zT expression, firstly proposed by A. F. Ioffe [27]. zT gives a direct measurement of the quality of the material for practical applications, and the figure of merit is clearly the central term for material engineering research. At a first glance the presence of the temperature in the expression of the figure of merit may be strange since T is not a material property, but an intensive parameter which partly defines the working conditions. Nevertheless, one should notice that, in terms of thermodynamic optimization, the material properties are nothing without considering the available exergy of the working system. This is achieved by introducing the temperature in the expression of the figure of merit which gives a reference to the exergy evaluation.

3. Heat & Entropy

Let us consider the coupled Onsager expressions:

$$\mathbf{J} = -\sigma_T \left(\frac{\nabla \mu_e}{e} \right) + \frac{\sigma_T S_N T^2}{e^2} \nabla \left(\frac{1}{T} \right) \tag{31}$$

$$\mathbf{J}_Q = -T \sigma_T S_N \left(\frac{\nabla \mu_e}{e} \right) + \left[\frac{T^3}{e^2} \sigma_T S_N^2 + T^2 \kappa_J \right] \nabla \left(\frac{1}{T} \right) \tag{32}$$

We can combine both equations to get

$$\mathbf{J}_Q = T S_N \mathbf{J} + T^2 \kappa_J \nabla \left(\frac{1}{T} \right) \tag{33}$$

where we identify a conductive term, proportional to $\nabla \left(\frac{1}{T} \right)$, and a “Peltier” term, proportional to \mathbf{J} :

$$\mathbf{J}_{Q_{\text{cond}}} = T^2 \kappa_J \nabla \left(\frac{1}{T} \right) \tag{34}$$

$$\mathbf{J}_{Q_{\text{pelt}}} = T S_N \mathbf{J} \tag{35}$$

This Peltier heat transported because of the thermoelectric effects results in the effect commonly attributed to Peltier: the heat observed at an inhomogeneous junction due to the thermoelectric effects.

3.1. Volumetric Heat Production

The volumetric heat production can be estimated from the total energy flux

$$\mathbf{J}_E = \mathbf{J}_Q + \frac{\mu_e}{e} \mathbf{J}$$

According to energy and particle conservation we have

$$\nabla \cdot \mathbf{J}_E = 0 \quad \text{and} \quad \nabla \cdot \mathbf{J} = 0 \quad (36)$$

Then

$$\nabla \cdot \mathbf{J}_Q = -\frac{\nabla \mu_e}{e} \cdot \mathbf{J}$$

Since the electrical field is $\mathbf{E} = -\frac{\nabla \mu_e}{e}$, we find

$$\nabla \cdot \mathbf{J}_Q = \mathbf{E} \cdot \mathbf{J} . \quad (37)$$

This summarizes the possible transformation of the energy since it shows that heat can be produced by the degradation of the electrochemical potential μ_e , and that electrical power can also be extracted from heat.

3.2. Entropy Production Density

If we consider the entropy flux density, we can calculate the entropy production ν_S from

$$\nu_S = \nabla \cdot \mathbf{J}_S = \nabla \cdot \left(\frac{\mathbf{J}_Q}{T} \right) = \nabla \cdot \left(\frac{1}{T} \right) \cdot \mathbf{J}_Q + \frac{1}{T} \nabla \cdot \mathbf{J}_Q$$

to get

$$\nu_S = \nabla \cdot \left(\frac{1}{T} \right) \cdot \mathbf{J}_Q - \frac{\nabla \mu_e}{eT} \cdot \mathbf{J} \quad (38)$$

As shown above, the entropy production is due to non-isothermal heat transfer and electrical Joule production. The previous expression can be rewritten in the form

$$\nu_S = \nabla \cdot \left(\frac{1}{T} \right) \cdot \mathbf{J}_E + \nabla \cdot \left(-\frac{\mu_e}{T} \right) \cdot \mathbf{J}_N \quad (39)$$

In this form, we get the illustration of one major result of the Onsager description: The total entropy production is given by the summation of the force-flux products,

$$\nu_S = \nabla \cdot \mathbf{J}_S = \Sigma \overrightarrow{\text{force}} \cdot \overrightarrow{\text{flux}} \quad (40)$$

This is a very general result of the Onsager theory. When deriving the entropy production according to Onsager kinetic expressions, the constraint of minimal entropy production leads to a final expression where the overall entropy production is directly given by the sum of the products of forces and the fluxes.

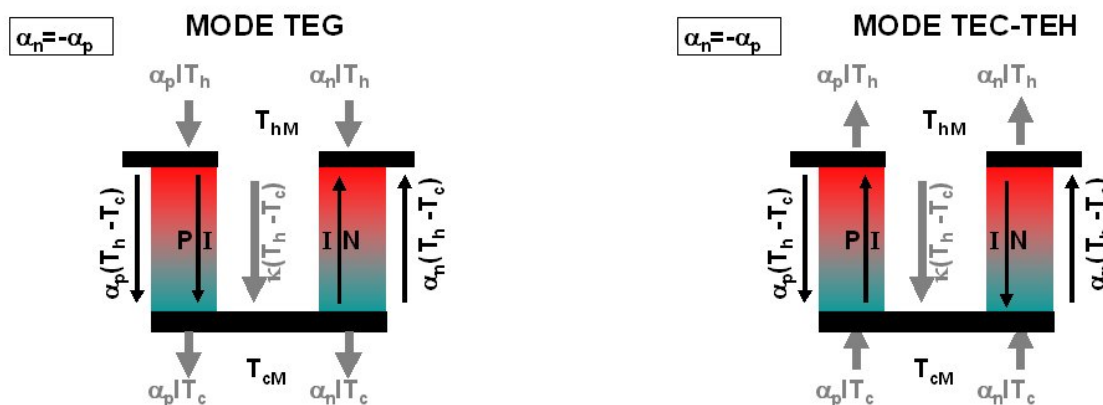
4. Thermoelectric Generator, Cooler, and Heater

From the practical point of view, the thermoelectric materials can be used for three applications:

- Thermoelectric heater: TEH.
- Thermoelectric cooler: TEC.
- Thermoelectric generator: TEG.

In all these configurations, the *p*- and *n*-bars of thermoelectric materials are polarized by thermal potential (temperature) or by the electrical potential. For TEH and TEC configuration, a voltage difference is applied through the structure, leading to a control of the temperature difference. For a TEG configuration a temperature difference is applied leading to the control of an external voltage difference. All three configurations are summarized in Figure 3, where the thermal processes are written in grey and the electrical processes in black.

Figure 3. TE applications (colour online).



We recognize the different potential differences:

- $\alpha_{n,p} (T_h - T_c)$: Seebeck voltage,
- $T_h - T_c$: temperature difference,

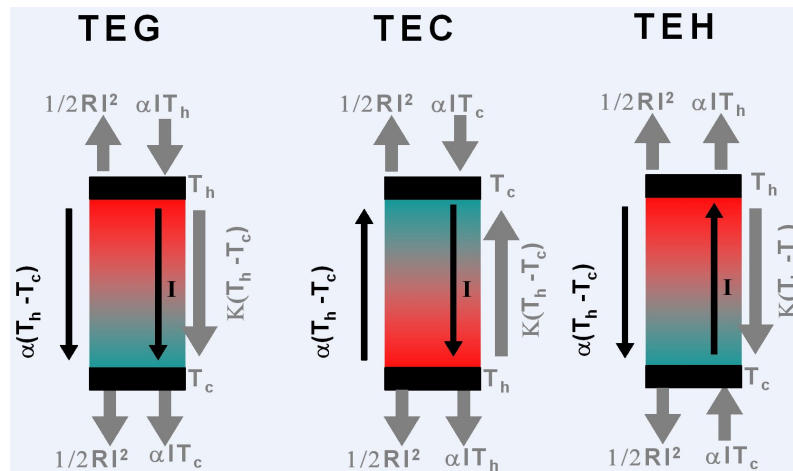
and also the different power terms:

- $\alpha_{n,p} T_{out} I$: Peltier heat flow.
- $K_{n,p} \Delta T$: conductive heat flow [113].

In order to simplify the derivation of the equations we restrict now the study to one “leg” of length *L* and *p*-type material with positive Seebeck coefficient [114]. Then, the previous picture changes into the Figure 4.

One can see that the TEG and TEC configurations appear to be very similar except that the imposed potentials differ since temperature difference is imposed for TEG and voltage difference for TEC.

Figure 4. Single-element devices.



At this point we would like to draw attention to the fact that there are different ways to model the three TE applications within the framework of a one-dimensional model, see e.g., [65], p. 489, and [115,116]. We recall here the results for the Constant Properties Model (CPM), see e.g., [27,115–117]. The temperature profile is a parabolic one and results from the thermal energy balance, see Section 5.4.; we have

$$T''(x) = -c_o \Rightarrow T(x) = -\frac{c_o}{2} x^2 + c_1 x + T_a \tag{41}$$

with $c_o = \frac{J^2}{\sigma_T \kappa_J}$, $c_1 = \frac{T_s - T_a}{L} + \frac{c_o}{2} L$

with boundary conditions of the first kind for a leg of length L ($0 \leq x \leq L$) and constant cross-sectional area A_c : $T(0) = T_a$ (temperature of the heat-absorbing side of the element, index a , which is the hot side for TEG but the cold side for TEC), $T(L) = T_s$ (temperature of the heat-sink side, index s , which is the cold side for TEG but the hot side for TEC). The analytical solution is discussed in detail, e.g., in [115].

From Equation (41), we find the temperature gradients at both element sides

$$\left(\frac{dT}{dx}\right)_{x=0} = \frac{T_s - T_a}{L} + \frac{c_o}{2} L, \quad \left(\frac{dT}{dx}\right)_{x=L} = \frac{T_s - T_a}{L} - \frac{c_o}{2} L \tag{42}$$

Note that $\kappa_J c_o L$ represents the density of Joule heating because we have within the framework of CPM: $I^2 R_{in}/A_c = J^2 R_{in} A_c = J^2 L/\sigma_T = \kappa_J c_o L$ with the isothermal (and internal) Ohmic resistance $R_{in} = L/(\sigma_T A_c)$. Consequently, the appropriate conductive heat fluxes are

$$J_Q(0) - \alpha T_a J = -\kappa \frac{T_s - T_a}{L} - J^2 \frac{L}{2 \sigma_T}$$

$$J_Q(L) - \alpha T_s J = -\kappa \frac{T_s - T_a}{L} + J^2 \frac{L}{2 \sigma_T} \tag{43}$$

Obviously, the mean temperature gradient $\Delta T/L$ is overlaid by Joule heating which is symmetrically distributed [118] over the length of the TE element.

Written with global values ($I = J A_c$, $K = \kappa J A_c/L$ etc.), we find from Equation (43) for the thermal power input $Q_a = A_c J_Q(0)$ at the absorbing side $x = 0$ (index a)

$$Q_a = \alpha T_a I - \frac{1}{2} I^2 R_{in} - K(T_s - T_a) \tag{44}$$

For inhomogeneous TE devices $Z = \alpha^2/(R_{in}K)$ is used to approximate the “device- Z ”. The device- Z is equal to the material’s figure of merit z for an ideal single-element device without parasitic losses within the framework of the CPM, as well as within the symmetric CPM model where the n -leg and p -leg have equal properties with opposite Seebeck.

Now we can derive the expressions for the three configurations within the framework of a global description. It was introduced by Altenkirch [11] and often used in technological applications as primarily considered by Ioffe [27] and Goldsmid [119]. For sake of simplification we use the load ratio $M = R_{load}/R_{in}$ for TEG. Then, as we will see, the expressions for the maximal power and maximal efficiencies lead to different values of the M parameter in the following summary of formulae.

4.1. Thermoelectric Generator

We are using here $T_h = T_a$, $T_c = T_s$ and $Q_{in} = Q_a$, $Q_{out} = Q_s$, respectively.

- Incoming thermal power:

$$Q_{in} = \alpha T_h I - \frac{1}{2} R_{in} I^2 + K (T_h - T_c)$$

- Outgoing thermal power:

$$Q_{out} = \alpha T_c I + \frac{1}{2} R_{in} I^2 + K (T_h - T_c)$$

- Electrical power produced:

$$P_{pro} = Q_{in} - Q_{out} = \alpha I (T_h - T_c) - R_{in} I^2$$

- Open voltage:

$$V_0 = \alpha (T_h - T_c)$$

Considering a resistor of resistance R_{load} connected to the TEG, we now define the load ratio $M = R_{load}/R_{in}$. Then we get the expressions of the output voltage and current

$$V_{out} = V_0 \frac{R_{load}}{R_{in} + R_{load}} = V_0 \frac{M}{1 + M} \tag{45}$$

$$I_{out} = \frac{V_0}{R_{in} + R_{load}} = \frac{V_0}{R_{in}(1 + M)} \tag{46}$$

and

$$P_{pro} = \frac{V_0^2}{R_{in}} \frac{M}{(M + 1)^2} \tag{47}$$

Then the efficiency can be expressed in a compact form,

- Efficiency:

$$\eta = \frac{P_{pro}}{Q_{in}} = \frac{\Delta T}{T_h} \frac{M}{M + 1 + \frac{(M+1)^2}{ZT_h} - \frac{1}{2} \frac{\Delta T}{T_h}} \quad \text{with} \quad \frac{1}{Z} = \frac{K R_{in}}{\alpha^2} \tag{48}$$

As we can notice the efficiency is the product of the reversible Carnot efficiency $\eta_C = \frac{\Delta T}{T_h} = \frac{T_h - T_c}{T_h}$ with the irreversible factor $M / \left(M + 1 + \frac{(M+1)^2}{ZT_h} - \frac{1}{2} \frac{\Delta T}{T_h} \right)$.

- Maximal efficiency:

From the derivation $\frac{\partial \eta}{\partial M} = 0$, we get after a few algebra steps

$$\eta_{\max} = \eta_c \frac{M_\eta - 1}{M_\eta + \frac{T_c}{T_h}} \tag{49}$$

with $M_\eta = \sqrt{1 + Z T_m}$ where $T_m = (T_h + T_c)/2$.

- Maximal electrical power output:

$$\begin{aligned} \frac{\partial P_{\text{pro}}}{\partial I} = 0 &= \alpha (T_h - T_c) - 2R_{\text{in}}I \\ I_P^{\max} &= \frac{\alpha (T_h - T_c)}{2 R_{\text{in}}} = \frac{V_0}{2 R_{\text{in}}} \end{aligned}$$

The last equation tells us that the maximal power output is obtained when the electrical load resistance R_{load} is equal to the internal resistance of the TEG. Then the maximal output power is obtained for $M_P = M = 1$. The maximal power expression reduces to

$$P_{\text{pro}}^{\max} = \frac{\alpha^2 \Delta T^2}{4 R_{\text{in}}} \tag{50}$$

One can notice that the condition for maximal efficiency ($M_\eta = \sqrt{1 + Z T_m}$) and maximal output power ($M_P = 1$) are different. This means that given a fabricated TE device where the geometric lengths and areas are fixed, more power will be produced if additional heat is supplied and higher current drawn than in the maximum efficiency configuration. However, when designing an optimal device for a particular application, the optimum design will have the geometry and current for maximum efficiency because this will provide more power with the same designed heat input.

4.2. Thermoelectric Cooler

We are using here $T_c = T_a$, $T_h = T_s$ and $Q_{\text{in}} = Q_a$, $Q_{\text{out}} = Q_s$, respectively.

- Incoming thermal power:

$$Q_c = \alpha T_c I - \frac{1}{2} R_{\text{in}} I^2 - K (T_h - T_c) \tag{51}$$

- Outgoing thermal power:

$$Q_{\text{rej}} = \alpha T_h I + \frac{1}{2} R_{\text{in}} I^2 - K (T_h - T_c) \tag{52}$$

- Consumed electrical power:

$$P_{\text{rec}} = Q_{\text{rej}} - Q_c = \alpha (T_h - T_c) I + R_{\text{in}} I^2$$

- Maximal cooling power:

$$I_{Q_c}^{\max} = \frac{\alpha T_c}{R_{\text{in}}} \tag{53}$$

$$Q_c^{\max} = \frac{1}{2} \frac{\alpha^2 T_c^2}{R_{in}} - K (T_h - T_c) = K \left(\frac{1}{2} T_c^2 Z - (T_h - T_c) \right) \tag{54}$$

One can notice that the maximal cooling power is directly driven by the figure of merit of the material and of the device, respectively.

- Coefficient of performance φ_c [120]:

$$\varphi_c = \frac{Q_c}{P_{rec}} = \frac{\alpha T_c I - \frac{1}{2} R_{in} I^2 - K (T_h - T_c)}{\alpha (T_h - T_c) I + R_{in} I^2} \tag{55}$$

- Maximal φ_c :

$$\frac{\partial \varphi_c}{\partial V_0} = 0 \quad \text{with } V_0 = \alpha(T_h - T_c) \text{ gives:}$$

$$\varphi_c^{\max} = \frac{T_c}{(T_h - T_c)} \frac{\sqrt{1 + ZT_m} - \frac{T_h}{T_c}}{\sqrt{1 + ZT_m} + 1} \tag{56}$$

V_0 is open voltage, a specific value of \mathcal{V} . The Carnot factor $\varphi_{Car} = \frac{T_c}{(T_h - T_c)}$ is the reversible term of φ_c^{\max} . The second term contains the irreversible contributions, $(\sqrt{1 + ZT_m} - \frac{T_h}{T_c}) / (\sqrt{1 + ZT_m} + 1)$

It should be noticed that Equation (56) is similar to the expression obtained for the TEG configuration, see Equation (49). Both formulae are well-known and often written as [27,119,121,122]

$$\eta_{\max} = \frac{T_h - T_c}{T_h} \frac{\sqrt{1 + ZT_m} - 1}{\sqrt{1 + ZT_m} + T_c/T_h} \tag{57}$$

and

$$\frac{1}{\varphi_c^{\max}} = \frac{T_h - T_c}{T_c} \frac{\sqrt{1 + ZT_m} + 1}{\sqrt{1 + ZT_m} - T_h/T_c} \tag{58}$$

making a convenient definition of the device figure of merit ZT (the exact value of which will depend on which equation is used and the temperature range). Moreover, maximum efficiency or φ are only obtained under specific working conditions, and practical applications usually do not exactly fulfill these conditions!

- Maximum cooling

The maximum temperature difference is achieved for $Q_c^{\max} = 0$ and hence for $\varphi_c = 0$. In this case we get from Equation (54)

$$\Delta T_{\max} = (T_h - T_c)_{\max} = \frac{1}{2} Z T_c^2 \tag{59}$$

4.3. Thermoelectric Heater

- Incoming thermal power:

$$Q_w = \alpha T_h I + \frac{1}{2} R_{in} I^2 - K (T_h - T_c) \tag{60}$$

- Outgoing thermal power:

$$Q_{\text{rej}} = \alpha T_c I - \frac{1}{2} R_{\text{in}} I^2 - K (T_h - T_c) \tag{61}$$

- Consumed electrical power:

$$P_{\text{rec}} = Q_w - Q_{\text{rej}} = \alpha (T_h - T_c) I + R_{\text{in}} I^2 \tag{62}$$

- Coefficient of performance:

$$\varphi_w = \frac{Q_w}{P_{\text{rec}}} = \frac{\alpha T_h I + \frac{1}{2} R_{\text{in}} I^2 - K (T_h - T_c)}{\alpha (T_h - T_c) I + R_{\text{in}} I^2} \tag{63}$$

- Maximal φ_w :

$$\varphi_w^{\text{max}} = \frac{T_h}{(T_h - T_c)} \left(1 - 2 \frac{\sqrt{1 + ZT_m} - 1}{ZT_h} \right) \tag{64}$$

The Carnot factor for φ is here $\varphi_{\text{Car}} = \frac{T_h}{(T_h - T_c)}$, whereas the irreversible contribution is given by the second term.

5. The General Conductivity Matrix

As we have seen from Ohm’s law and Fourier’s law, the kinetic coefficients can be written in the form of conductances and it is tempting to express the force-flux previous expressions in the form of a general conductance matrix. Such a description has been derived in a very general way by Callen and Greene in 1952 [110,123]. The complete derivation is out of the scope of this presentation and we only consider here the basic derivation of a general conductivity matrix.

5.1. Derivation of the Conductivity Matrix

Starting from Equation (4) and using the kinetic coefficients listed in Section 2.6 we have

$$\begin{bmatrix} \mathbf{J}_N \\ \mathbf{J}_Q \end{bmatrix} = \begin{bmatrix} \frac{T}{e^2} \sigma_T & \frac{T^2}{e^2} \sigma_T S_N \\ \frac{T^2}{e^2} \sigma_T S_N & T^2 \kappa_E \end{bmatrix} \begin{bmatrix} -\frac{1}{T} \nabla(\mu_e) \\ \nabla(\frac{1}{T}) \end{bmatrix}$$

We know that the electrical field and the electrical current flux are given by

$$\mathbf{E} = -\frac{\nabla \mu_e}{e} \quad \text{and} \quad \mathbf{J} = e \mathbf{J}_N$$

If we consider the local expansion $\nabla (\frac{1}{T}) = -\frac{1}{T^2} \nabla T$, we finally get

$$\begin{bmatrix} \mathbf{J} \\ \mathbf{J}_Q \end{bmatrix} = \begin{bmatrix} \sigma_T & \alpha \sigma_T \\ T \alpha \sigma_T & \kappa_E \end{bmatrix} \begin{bmatrix} \mathbf{E} \\ -\nabla T \end{bmatrix}$$

The electrical and heat fluxes can be described now through the general conductivity matrix

$$[\sigma] = \begin{bmatrix} \sigma_T & \alpha \sigma_T \\ T \alpha \sigma_T & \kappa_E \end{bmatrix}$$

Notice that the Seebeck coefficient α appears as the coupling term between the electrical and thermal processes. In a material with $\alpha = 0$ the conductivity matrix reduces to a diagonal form $\begin{bmatrix} \sigma_T & 0 \\ 0 & \kappa_E \end{bmatrix}$ where Ohm’s law and Fourier’s law are then decoupled. In other words the Seebeck coefficient, or more precisely the entropy per carrier, is the “tuning parameter” of the coupling between charge and heat transport. Notice that these elementary considerations may open the door for a description of non-homogeneous TE material as a serial-parallel network of local homogeneous elements, and for the optimization of Functionally Graded Material (FGM) using the transport matrix. First results have been published in [124].

5.2. The Peltier-Thomson Coefficient

In the previous paragraphs we have considered the volumetric heat transformation from the calculation of the divergence of the heat flux $\nabla \cdot \mathbf{J}_Q$. We propose now to analyze its different terms. First, by elimination of the electric field \mathbf{E} from the previous set of equations we get

$$\mathbf{J}_Q = \alpha T \mathbf{J} - \kappa_J \nabla T \tag{65}$$

and the divergence of the heat flux becomes

$$\begin{aligned} \nabla \cdot \mathbf{J}_Q &= \nabla \cdot (\alpha T \mathbf{J} - \kappa_J \nabla T) \\ &= T \mathbf{J} \cdot \nabla \alpha + \alpha \nabla T \cdot \mathbf{J} + \alpha T \nabla \cdot \mathbf{J} + \nabla \cdot (-\kappa_J \nabla T) \end{aligned} \tag{66}$$

where we find four terms which can be identified:

- $\alpha T \nabla \cdot \mathbf{J}$: equals zero due to particle conservation,
- $T \mathbf{J} \cdot \nabla \alpha$: “Peltier-Thomson” term,
- $\mathbf{J} \cdot \alpha \nabla T = \mathbf{J} \cdot \left(\mathbf{E} - \frac{1}{\sigma_T} \mathbf{J} \right) = \mathbf{J} \cdot \mathbf{E} - \frac{J^2}{\sigma_T}$: electrical work production and dissipation,
- $\nabla \cdot (-\kappa_J \nabla T)$: change in thermal conduction due to heat produced or absorbed.

To sum up, the sources of the heat flux are

$$\nabla \cdot \mathbf{J}_Q = T \mathbf{J} \cdot \nabla \alpha + \mathbf{J} \cdot \mathbf{E} - \frac{J^2}{\sigma_T} - \nabla \cdot (\kappa_J \nabla T) \tag{67}$$

Most of these terms are common, but less intuitive is the Peltier–Thomson term which is now considered.

5.3. The Peltier–Thomson Term

We will show now that the $T \mathbf{J} \cdot \nabla \alpha$ term contains both the Thomson contribution (local temperature gradient effect), and the Peltier contribution (isothermal spatial gradient effect). Using the equivalence $\Pi = \alpha T$ we have

$$T \mathbf{J} \cdot \nabla \alpha = T \mathbf{J} \cdot \nabla \left(\frac{\Pi}{T} \right) = T \mathbf{J} \cdot \left(\frac{1}{T} \nabla \Pi - \frac{1}{T^2} \Pi \nabla T \right) = \mathbf{J} \cdot (\nabla \Pi - \alpha \nabla T) \tag{68}$$

Then, the traditional separation of the Peltier and Thomson contribution is artificial since they both refer to the same physics of the gradient of the entropy per particle, the temperature driven gradient or the spatially driven gradient. The isothermal configuration leads to the Peltier expression meanwhile a spatial gradient gives the Thomson result:

- Pure Peltier, isothermal junction between two materials:

$$\mathbf{J} \cdot (\nabla\Pi - \alpha\nabla T) = \mathbf{J} \cdot (\nabla\Pi)$$

- Thomson, homogeneous material under temperature gradient:

$$\mathbf{J} \cdot (\nabla\Pi - \alpha\nabla T) = \mathbf{J} \cdot \left(\frac{d\Pi}{dT} - \alpha \right) \nabla T = \tau \mathbf{J} \cdot \nabla T \tag{69}$$

with

$$\nabla\Pi = \frac{d\Pi}{dT} \nabla T \quad \text{and} \quad \tau = \frac{d\Pi}{dT} - \alpha \tag{70}$$

and the heat flux divergence takes the form

$$\nabla \cdot \mathbf{J}_Q = \tau \mathbf{J} \cdot \nabla T + \mathbf{J} \cdot \mathbf{E} - \frac{J^2}{\sigma_T} - \nabla \cdot (\kappa_J \nabla T) \tag{71}$$

If we consider a configuration $\kappa = \text{const}$, then Equation (71) reduces to

$$\nabla \cdot \mathbf{J}_Q = \tau \mathbf{J} \cdot \nabla T + \mathbf{J} \cdot \mathbf{E} - \frac{J^2}{\sigma_T} - \kappa_J \nabla^2 T \tag{72}$$

As one can notice, the Peltier and Thomson both refers to the gradient $\nabla\alpha$. It is worth noticing that the isothermal configuration for the Peltier expression, and the temperature gradient configuration for the Thomson effect, correspond to specific chosen conditions. With another set of conditions, one can obtain other definitions. For example, due to the position-dependent Seebeck coefficient, Peltier heat can be considered to be absorbed or released inside the active material. It is then referred to as the distributed Peltier effect or the extrinsic Thomson effect [125–127].

5.4. Local Energy Balance

Using the expression $\nabla \cdot \mathbf{J}_Q = \mathbf{E} \cdot \mathbf{J}$, see Equation (37), the local energy balance can be expressed from Equation (72) [128]:

$$\nabla \cdot \mathbf{J}_Q - \mathbf{E} \cdot \mathbf{J} = \kappa_J \nabla^2 T + \frac{J^2}{\sigma_T} - \tau \mathbf{J} \cdot \nabla T = 0 \tag{73}$$

It should be noticed that this derivation does not need any assumption concerning the behavior of the system, in equilibrium or not. In the transient configuration the energy balance equation should be corrected using $\rho_m C_p$ where C_p is the heat capacity and ρ_m the volumetric mass:

$$\rho_m C_p \frac{\partial T}{\partial t} + \nabla \cdot \mathbf{J}_Q = \mathbf{E} \cdot \mathbf{J} \longrightarrow \kappa_J \nabla^2 T + \frac{J^2}{\sigma_T} - \tau \mathbf{J} \cdot \nabla T = \rho_m C_p \frac{\partial T}{\partial t} \tag{74}$$

In this form, the local energy balance has the general form of a continuity Equation [117]. One-dimensional models are often used, see, e.g., [65,115,116]. Even in one dimension, the addition of time dependence can induce additional effects. For example, the spatial separation of Peltier cooling from Joule heating enables additional transient cooling when a cooler is pulsed [129]. The reader may find some more information and insights about transient effects in thermoelectrics in [87,88,130–142].

6. Relative Current and Thermoelectric Potential

Until now we have not really taken into account the working conditions of the TE system. Like any working engine, a thermoelectric device should be correctly driven in order to provide work in the best conditions. Then a precise control of the applied thermodynamic potentials (or fluxes) is needed in order to get a correct use of the potentialities of the thermoelectric material. Since the thermoelectric process implies the coupling of the heat and electrical fluxes, these two fluxes should both be driven optimally. This important question has been addressed by J. Snyder and co-workers in 2002 and 2003. They derived two main parameters: the relative current and the thermoelectric potential [143,144].

6.1. Relative Current and Thermoelectric Potential

The relative current density is defined by the ratio of electrical current density \mathbf{J} to the purely conductive fraction of the heat flux with respect to the flow direction of $\mathbf{J} = J \mathbf{n}$

$$u = -\frac{\mathbf{J} \cdot \mathbf{n}}{\kappa_J \nabla T \cdot \mathbf{n}} \quad \text{or} \quad 1/u = -\frac{\kappa_J \nabla T \cdot \mathbf{J}}{\mathbf{J} \cdot \mathbf{J}} \tag{75}$$

From Equation (65) the heat flow becomes

$$\mathbf{J}_Q = \alpha T \mathbf{J} + \frac{\mathbf{J}}{u} = \Phi \mathbf{J}, \quad \Phi = \left(\alpha T + \frac{1}{u} \right) \tag{76}$$

where Φ is the “thermoelectric potential”.

The heat and carrier fluxes are now directly connected by the thermoelectric potential, whereby we generally assume here parallelity of electrical current and heat flow [145]. This expression is fundamental since it allows us to derive the principle results of the thermodynamics of thermoelectricity directly from it. According to the previous definitions, the volumetric heat production ν_q becomes (with $\nabla \cdot \mathbf{J} = 0$)

$$\nu_q = \nabla \cdot \mathbf{J}_Q = \nabla \cdot (\Phi \mathbf{J}) = \nabla \Phi \cdot \mathbf{J} = \mathbf{J} \cdot \nabla \left(T\alpha + \frac{1}{u} \right) \tag{77}$$

Note that $\nabla \cdot \mathbf{J}_Q = \mathbf{J} \cdot \mathbf{E}$, see Equation (37), and $\mathbf{E} = -\frac{\nabla \mu_e}{e}$, see Equation (6). Then, we find

$$\mathbf{E} = \nabla \Phi = -\nabla \mu_e / e \implies \mu_e = -e(\Phi - \Phi_0) \tag{78}$$

which means that the electric field \mathbf{E} can be calculated on a phenomenological level from the gradient of the TE potential Φ , or alternatively, by the negative gradient $-\nabla \mu_e / e$ when referring to a TE system by taking into account its solid-state physics nature. For details we recommend the reading of Domenicali’s review [24].

Since the heat production term $\mathbf{J} \cdot \nabla \left(\frac{1}{u} \right)$ directly reduces the efficiency, it becomes evident that the maximum efficiency coincides with the minimization of $\nabla \left(\frac{1}{u} \right)$. This is obtained for a specific value of $u_{\text{opt}} = s$, where s is called the “compatibility factor” (see next section).

Considering the entropy flux we get $\mathbf{J}_S = \frac{1}{T} \left(\alpha T + \frac{1}{u} \right) \mathbf{J} = \frac{\Phi}{T} \mathbf{J}$, and the expression of the volumetric entropy production becomes

$$\nu_S = \nabla \cdot \mathbf{J}_S = \mathbf{J} \cdot \nabla \left(\frac{\Phi}{T} \right) = \frac{\nu_q}{T} + \mathbf{J}_Q \cdot \nabla \left(\frac{1}{T} \right) \tag{79}$$

This expression is in agreement with the Onsager formulation of the entropy production as the summation of the flux-force products, see Equation (39), which here reduces to a single product since Φ is a compact expression of the thermodynamic potentials. For a given material the thermoelectric potential gives a direct measurement of the total volumetric heat and entropy production by the respective degradation of Φ and $\frac{\Phi}{T}$.

6.2. Thermoelectric Potential and Local Reduced Efficiency for a Thermogenerator

As an example, let us calculate the local efficiency of a thermogenerator (TEG) [146] which is defined as the ratio of the products of conjugated forces and fluxes [144]. In this context it should be noticed that the power output in a volume dV is given by the dot product $\pi_{el} = \mathbf{j} \cdot \mathbf{E}$, also denoted as differential electrical power, and that the net differential power output [147] is given by $-\pi_{el}$, see also [148]. Using Equations (37) and (1) we get $\mathbf{E} \cdot \mathbf{J} = \nabla \cdot \mathbf{J}_Q = T \nu_S + \mathbf{J}_S \cdot \nabla T$ which leads to the expression of the reduced efficiency

$$\eta_r = \frac{\mathbf{E} \cdot \mathbf{J}}{\mathbf{J}_S \cdot \nabla T} = \frac{\pi_{el}}{\pi_{el} - T \nu_S} = \frac{1}{1 - \frac{T \nu_S}{\pi_{el}}} = \frac{1}{1 + \frac{T \nu_S}{|\pi_{el}|}} \tag{80}$$

Thus, the efficiency is expressed in terms of the ratio of entropy production to the net power output density. This is consistent with Clingman’s results using thermodynamic arguments, see [49,50]. In an irreversible configuration the $T \nu_S$ term tends to reduce the efficiency. In the ideal case of a reversible process the entropy production is zero, then the work production $\mathbf{E} \cdot \mathbf{J} = \nabla \cdot \mathbf{J}_Q = T \nabla \cdot \mathbf{J}_S + \mathbf{J}_S \cdot \nabla T$ reduces to $\mathbf{E} \cdot \mathbf{J} = \mathbf{J}_S \cdot \nabla T$ and the reduced efficiency is $\eta_r = 1$, which means that the Carnot efficiency is reached. It should be noticed, however, that even today’s best available TE materials do not reach 20 % of the Carnot efficiency.

Let us now consider the introduction of the thermoelectric potential Φ into the calculation of the reduced efficiency, which can be written as

$$\eta_r = \frac{\mathbf{E} \cdot \mathbf{J}}{\mathbf{J}_S \cdot \nabla T} = \frac{\nabla \cdot \mathbf{J}_Q}{\frac{\mathbf{J}_Q}{T} \cdot \nabla T} = \frac{T \nabla \Phi \cdot \mathbf{J}}{\Phi \nabla T \cdot \mathbf{J}} \tag{81}$$

and which corresponds to the relative variation of the thermodynamic potential $\frac{\nabla \Phi}{\Phi}$ when changing the “thermic” potential $\frac{\nabla T}{T}$. This is coherent with a general definition of the efficiency of an out-of-equilibrium thermodynamic process as a coupled fluctuating system [101].

Further, we can rewrite the relative current with $\mathbf{J} = \sigma_T \mathbf{E} - \sigma_T \alpha \nabla T$ and $\mathbf{E} = \nabla \Phi$ [146]

$$u = -\frac{\mathbf{J} \cdot \mathbf{J}}{\kappa_J \nabla T \cdot \mathbf{J}} = -\frac{\sigma_T (\mathbf{E} - \alpha \nabla T) \cdot \mathbf{J}}{\kappa_J \nabla T \cdot \mathbf{J}} = -\frac{z \nabla \Phi \cdot \mathbf{J}}{\alpha^2 \nabla T \cdot \mathbf{J}} + \frac{z}{\alpha} \tag{82}$$

Introducing the expression of the reduced efficiency, see Equation (81), we finally get with Φ given by Equation (76)

$$u = \frac{z}{\alpha} \left[-\left(1 + \frac{1}{\alpha T u}\right) \eta_r + 1 \right] \tag{83}$$

Solving for η_r , the reduced efficiency of a TEG leg becomes [144]

$$\eta_r = \frac{\frac{u\alpha}{z} \left(1 - \frac{u\alpha}{z}\right)}{\left(\frac{u\alpha}{z} + \frac{1}{zT}\right)} = \frac{1 - \frac{\alpha}{z(\Phi - T\alpha)}}{1 + \frac{z(\Phi - T\alpha)}{zT\alpha}} \tag{84}$$

This classical expression of the reduced efficiency presents a maximum for the compatibility factor $u_{\text{opt}} = s = \frac{\sqrt{1+zT}-1}{\alpha T}$. In that case the optimal reduced efficiency becomes

$$\eta_{r,\text{opt}} = \frac{\sqrt{1+zT}-1}{\sqrt{1+zT}+1} = \left(2\frac{\Phi_{\text{opt}}}{\alpha T} - 1\right)^{-1} \quad (85)$$

where the equivalent optimal potential is

$$\Phi_{\text{opt}} = \left[T\alpha + \frac{1}{s}\right] = T\alpha \left[\frac{\sqrt{1+zT}}{\sqrt{1+zT}-1}\right] \quad (86)$$

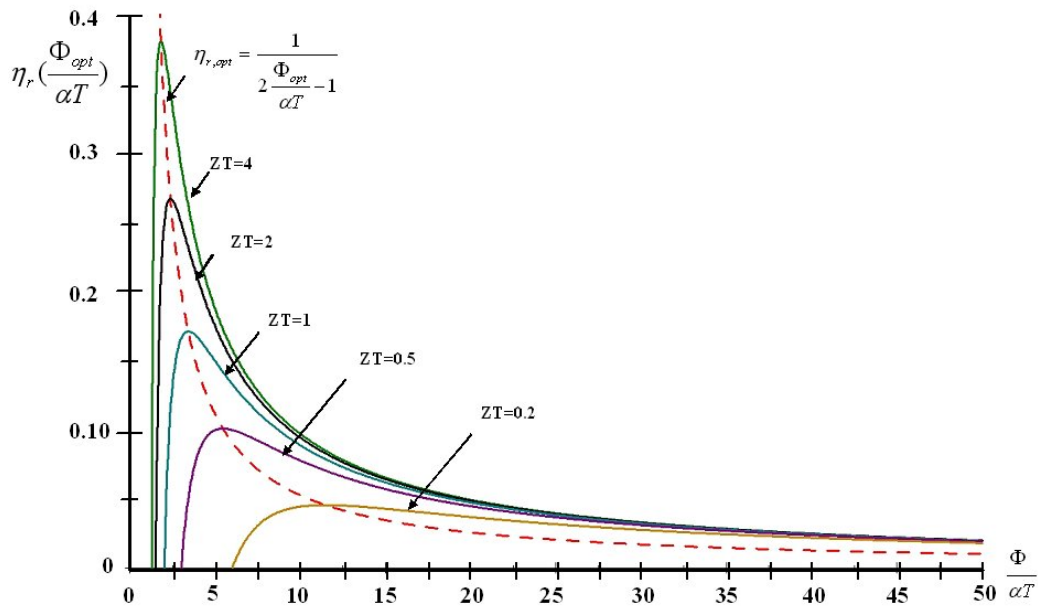
Since the maximum reduced efficiency coincides with minimal entropy production, we conclude that the optimal value of thermoelectric potential, Φ_{opt} , defines the best working conditions for the system. Therefore it is obvious that an optimal value Φ_{opt} is correlated to an optimal ratio between heat flux and electrical flux given by $u_{\text{opt}} = s$. To show this we plot the expression $\eta_r = f\left(\frac{\Phi}{T}\right)$ for various zT values, see Figure 5. One can notice that this Φ dependence becomes sharper as zT values increase. This is in agreement with the assumption that the proximity to reversibility implies a drastic control of the working contributions. This is obtained by a direct control of $\Phi = \Phi_{\text{opt}}$. As a consequence, it becomes possible to control the maximum reduced efficiency by keeping Φ near its optimal value $\Phi = \Phi_{\text{opt}}$. This approach extends the compatibility approach by adding a thermodynamic feedback by a direct measurement of the local entropy production $\nabla \cdot \mathbf{J}_S$. The expression of the irreversibility factor gives an insight into the sensitivity of the thermoelectric system to varying working conditions. It shows that for large zT this sensitivity becomes very high and strong reduction of the efficiency can rapidly occur.

Let us reconsider Φ as a tuning parameter of the working conditions of the thermodynamic system. We have two remarks. First, one can see that Φ contains, in a compact form, the values of the two intensive parameters of the system, temperature and electrochemical potential, which constitute the working conditions of the system. From the tuning of these two parameters the working conditions of the system can be optimized or not. Second, we consider processes where energy is exchanged in finite time [149]. As we know from finite time thermodynamics, the exchange of power cannot be achieved without an increase in entropy, without violation of potential continuity. As an illustration, the presence of thermal exchangers is needed to ensure the temperature continuity from the heat reservoir to the system. In other words, producing or exchanging power implies rejecting a certain amount of heat. In that way this optimal tuning of the potentials gives the minimal necessary heat rejection in order to get the best working conditions for the system.

6.3. Compatibility Approach

The importance of the compatibility approach has been demonstrated first for a segmented thermoelectric generator [67,143,144]. Snyder pointed out that, if the compatibility factors in segmented devices with given material differ by a factor of two or more, the maximum efficiency of a TEG is reduced (the device- ZT can in fact decrease rather than increase by segmentation even if the average zT is increased). Compatibility is thus of essential importance for a rational material selection in segmented devices.

Figure 5. Reduced efficiency $\eta_r = f(\frac{\Phi}{\alpha T})$ for TEG (irreversible factor).



Doubtless, the compatibility approach is an alternative to Ioffe’s global description which is very often used for technological applications, but is certainly not suitable for locally characterizing TE processes or even for local optimization purposes.

The advantage of using the relative current density is that the multidimensional TE problem can be reduced to a one-dimensional heat flow problem formulated in $u(T)$ where the governing equation can be evaluated from the thermal energy balance [144]

$$\frac{d}{dT} \left(\frac{1}{u} \right) = -T \frac{d\alpha}{dT} - u\rho\kappa \quad \text{or, alternatively} \quad u'(T) = \tau u^2 + \rho\kappa u^3 \tag{87}$$

with the Thomson coefficient $\tau(T) = T d\alpha/dT$. An analytical solution exists for constant material properties [116,144]. Basically, Equation (87) describes a homogeneous TE element with temperature dependent material properties, whereby (87) holds for both cases “pump up” ($T'(x) > 0$) and “pump down” ($T'(x) < 0$) [150]. Further note that TEG and TEC cases are only distinguished by the sign of $u(T)$ if the same (temperature dependent) material properties, the same current density, but reversed boundary temperatures T_a and T_s are applied ($T_a > T_s$ for TEG, but $T_a < T_s$ as usual for TEC).

The compatibility approach has been further developed in the successive works [116,151–153] and applied also to the Peltier cooler on the basis of a one-dimensional, steady-state and unifying model for TEG and TEC. It has been shown that a reduced coefficient of performance φ_r can also be derived for TEC [154]. Following [67], Section 9.2.2. and [116] we can conclude that the local performance of an infinitesimal segment of length dx with $dT = T'(x)dx$ is given by

$$\eta_{loc} = \frac{dT}{T} \eta_r \quad \text{and} \quad \varphi_{loc} = \frac{T}{dT} \varphi_r \tag{88}$$

where dT/T is the infinitesimal Carnot cycle factor for TEG and T/dT for TEC.

For directly comparing TEG and TEC, we find formally $\varphi_r = 1/\eta_r$ as a consequence of the underlying TE effects which are inverse to each other [116]. Because the Carnot cycle is a reversible process, the

reduced “efficiencies” η_r, φ_r play the role of an irreversibility factor which at least measures the distance to reversibility for both TEG and TEC due to a non perfect TE engine. Thus zT is a measure of how close to reversibility the system can come locally; while the compatibility factor defines the working conditions required to achieve the degree of reversibility allowable by the zT . The total efficiency η and the total coefficient of performance φ is obtained by summing up all local contributions all over the thermoelectric element in an integral sense. The integrals for η and φ are with respect to temperature [153]:

$$\ln(1 - \eta) = \int_{T_a}^{T_s} K [u(T), T] dT \quad \text{for TEG : } T_s \leq T \leq T_a \quad (89)$$

$$\ln \left(1 + \frac{1}{\varphi} \right) = \int_{T_a}^{T_s} K [u(T), T] dT \quad \text{for TEC : } T_a \leq T \leq T_s \quad (90)$$

where we have one kernel $K [u(T), T]$ for integrals of both generator and cooler elements

$$K(u, T) = \frac{1}{T} \eta_r(u, T) = \frac{1}{T} \frac{1}{\varphi_r(u, T)} = \frac{1}{T} \frac{u \frac{\alpha}{z} (1 - u \frac{\alpha}{z})}{u \frac{\alpha}{z} + \frac{1}{zT}} = \frac{\alpha}{z} \frac{(z - u\alpha)}{(u^{-1} + \alpha T)} \quad (91)$$

Note that $u(T)$ is different for TEG and TEC. Alternatively, the integral kernel K can be formulated with the TE potential Φ , see Equation (84). For this case, Snyder [67,144] has shown that η is simply given by the relative change of the thermoelectric potential; an analogous relation can be found for the coefficient of performance (see [116])

$$\eta = 1 - \frac{\Phi(T_s)}{\Phi(T_a)}, \quad \varphi = \left(\frac{\Phi(T_s)}{\Phi(T_a)} - 1 \right)^{-1} \quad (92)$$

This result points to the importance of the TE potential as a function of state: an optimized thermoelectric potential Φ_{opt} is correlated with a minimal entropy production which in turn leads to an optimal ratio between heat flux and electrical flux and thus a maximum performance value given by $u_{opt} = s$. Such TE elements are called self-compatible elements. Depending on the working conditions, the relation $\Phi(T_s)/\Phi(T_a) > T_s/T_a$ can be considered as a measure of how far TE elements operate from reversibility, for more information see [155].

The necessary condition for an extreme value leads to different compatibility factors for maximum efficiency of a TEG and maximum φ of a TEC; the reduced “efficiencies” η_r and φ_r present local extrema (maxima) for $u_{opt} = \frac{\sqrt{1+zT}-1}{\alpha T}$ for a TEG, but $u_{opt} = \frac{-\sqrt{1+zT}-1}{\alpha T}$ for a TEC [143,144]. Due to the definition of u , the compatibility factor for maximum φ of a TEC must be negative [156]. The optimal reduced efficiency for TEG and optimal reduced φ for TEC is $\eta_{r,opt} = \varphi_{r,opt} = \frac{\sqrt{1+zT}-1}{\sqrt{1+zT}+1}$ for both TEG and TEC, and the integrals for “fully” self-compatible performance η_{sc} and φ_{sc} are given by

$$\ln(1 - \eta_{sc}) = \int_{T_a}^{T_s} \frac{\eta_{r,opt}}{T} dT = \int_{T_a}^{T_s} \frac{1}{T} \frac{\sqrt{1+zT}-1}{\sqrt{1+zT}+1} dT \quad (93)$$

$$\ln \left(1 + \frac{1}{\varphi_{sc}} \right) = \int_{T_a}^{T_s} \frac{1}{T \varphi_{r,opt}} dT = \int_{T_a}^{T_s} \frac{1}{T} \frac{\sqrt{1+zT}+1}{\sqrt{1+zT}-1} dT \quad (94)$$

which is equivalent to Sherman’s notation [47,157]

$$\eta_{sc} = 1 - \exp \left(- \int_{T_s}^{T_a} \frac{1}{T} \frac{\sqrt{1+zT}-1}{\sqrt{1+zT}+1} dT \right), \quad (95)$$

$$\varphi_{sc} = \left[\exp \left(\int_{T_a}^{T_s} \frac{1}{T} \frac{\sqrt{1+zT}+1}{\sqrt{1+zT}-1} dT \right) - 1 \right]^{-1} \quad (96)$$

We expressly emphasize that the integrals (95) and (96) do not have extremal properties concerning the zT value. Analytical expressions of these integrals can be found for $z = \text{const.}$ as well as for $zT = \text{const.}$ For integral approximations, more theoretical background and historical notes we refer to [153,155].

7. Optimum Device Design and FGM

The ultimate objectives in TE research are to increase the performance and to reduce the cost of TE devices. Along with continuing to improve the material's figure of merit, the optimum design of TE systems is of particular importance. Whenever efficiency η or coefficient of performance φ is in focus, an irreversible thermodynamic analysis of the system is useful; already Clingman [49,50] set out to use entropy production to derive the optimum device design. This paper has presented a similar but improved approach. The novelty is to use the compatibility approach together with thermodynamic arguments, whereby the introduction of the TE potential opens up new opportunities for optimizing the performance of TE devices. Since this operation is equivalent to the adaptation of the thermal and electric impedance of the device, such a strategy also includes classical design parameters like the ratio of the length of an active TE element to its cross-sectional area [158–164]. Naturally, the concept of Functionally Graded Materials (FGM) [165–170] is an efficient way to achieve this impedance adaptation, and to further contribute to a gradual improvement of device performance. A central target of theoretical FGM studies is to elaborate recipes for optimum design of TE elements concerning the material [152,170,171], *i.e.*, to identify optimal profiles of the material coefficients α , σ_T , and κ_J . Ideally, it would be best to have a local criterion for optimizing global performance; currently local criteria are known for the efficiency of a thermogenerator and the coefficient of performance of a Peltier cooler [144,153]. However, global optimization requires constraints for the range of temperature dependent materials properties in available materials. In order to prevent global performance divergences in the optimization process, limits of the material properties have to be included in the process, be these upper limits for Seebeck $\alpha(T)$ and electric conductivity $\sigma_T(T)$ and a lower limit for the thermal conductivity $\kappa_J(T)$, or averages of the TE properties, of the power factor, or of the efficiency. Further results on material optimization will be presented in the chapter 4 of the first volume of the new CRC Handbook [169].

8. Conclusions

Using the Onsager–de Groot–Callen model we derive the complete expressions for the heat flux and electrical current density in a thermoelectric material. In particular, it is shown that the traditional Peltier and Thomson contributions can be expressed in a unique and compact form, only differing in the boundary conditions. Practical design expressions of thermogenerators and thermoelectric coolers and heaters can then be simply derived. Using the relative current density and the thermoelectric potential we reconsider the question of the optimal efficiency of a thermogenerator. It is shown that the best thermodynamic working conditions are obtained when the relative current density is equal to a specific value which directly depends on the material properties. This strongly influences the design of the thermoelectric devices since the thermoelectric materials should work under specific thermodynamic

conditions in terms of temperature and electrochemical potential differences. In particular, these working conditions can be considered and optimized using FGM.

Acknowledgements

The first author would like to thank the French CNRS “Programme Interdisciplinaire Energie”, and the ANR “Efficacité Energétique des Systèmes Industriels” for their support.

References

1. Seebeck, T.J. Ueber den Magnetismus der galvanischen Kette. Technical report for the Royal Prussian Academy of Science: Berlin, Germany, 1821.
2. Seebeck, T.J. Magnetische Polarisation der Metalle und Erze durch Temperatur-Differenz. Technical report for the Royal Prussian Academy of Science: Berlin, Germany, 1823.
3. Seebeck, T.J. Ueber die magnetische Polarisation der Metalle und Erze durch Temperatur-Differenz. *Annalen der Physik* **1826**, *82*, 1–20.
4. Seebeck actually misinterpreted the observed effect as a thermomagnetic coupling. The correct interpretation of the effect was given later by Oersted. Nevertheless, some authors consider Alessandro Volta to be at the origin of the discovery of this thermoelectric effect [172,173]. The introduction of additional effects due to a magnetic field into the Onsager relations is possible, see e.g. the Nernst effect and Ettinghausen effect [21,22,35,117].
5. Peltier, J.C.A. Nouvelles expériences sur la calorité des courants électrique. *Annales de Chimie et de Physique* **1834**, *56*, 371–386.
6. Thomson, W. On the Mechanical Theory of Thermo-electric Currents. *Trans. R. Soc. Edinburgh: Earth Sci.* **1851**, *3*, 91–98.
7. Kohlrausch, F. Ueber den stationären Temperaturzustand eines elektrisch geheizten Leiters. *Annalen der Physik* **1900**, *306*, 132–158.
8. Diesselhorst, H. Ueber das Problem eines elektrisch erwärmten Leiters. *Annalen der Physik* **1900**, *306*, 312–325.
9. Lord Rayleigh. On the thermodynamic efficiency of the thermopile. *Philosophical Magazine Series 5* **1885**, *20*, 361–363.
10. Altenkirch, E. Über den Nutzeffekt der Thermosäulen. *Physikalische Zeitschrift* **1909**, *10*, 560–580.
11. Altenkirch, E. Elektrothermische Kälteerzeugung und reversible elektrische Heizung. *Physikalische Zeitschrift* **1911**, *12*, 920–924.
12. The transport parameters are often used without subscripts: $\sigma \equiv \sigma_T$ is the isothermal conductivity and $\kappa \equiv \kappa_J$ the thermal conductivity under zero current.
13. Telkes, M. Technical Report for Westinghouse: Pittsburgh, PA, USA, 1938; R-94264-8.
14. Wood, C. Materials for thermoelectric energy conversion. *Rep. Prog. Phys.* **1988**, *51*, 459–539.
15. Telkes, M. The Efficiency of Thermoelectric Generators. I. *J. Appl. Phys.* **1947**, *18*, 1116–1127.
16. Telkes, M. Solar Thermoelectric Generators. *J. Appl. Phys.* **1954**, *25*, 765–777.
17. Telkes, M. Power Output of Thermoelectric Generators. *J. Appl. Phys.* **1954**, *25*, 1058–1059.

18. Onsager, L. Reciprocal Relations in Irreversible Processes. I. *Phys. Rev.* **1931**, *37*, 405–426.
19. Onsager, L. Reciprocal Relations in Irreversible Processes. II. *Phys. Rev.* **1931**, *38*, 2265–2279.
20. Onsager, L. Theories and Problems of Liquid Diffusion. *Ann. N.Y. Acad. Sci.* **1945**, *46*, 241–265.
21. Callen, H.B. The Application of Onsager's Reciprocal Relations to Thermoelectric, Thermomagnetic, and Galvanomagnetic Effects. *Phys. Rev.* **1948**, *73*, 1349–1358.
22. Callen, H.B. *On the theory of irreversible processes*. PhD thesis, Massachusetts Institute of Technology - (M.I.T.), Cambridge, MA, USA, 1947.
23. de Groot, S.R. *Thermodynamics of Irreversible Processes*; North-Holland Publishing Company: Amsterdam, The Netherlands, 1963.
24. Domenicali, C.A. Stationary Temperature Distribution in an Electrically Heated Conductor. *J. Appl. Phys.* **1954**, *25*, 1310–1311.
25. Joffe, A.F. The Revival of Thermoelectricity. *Sci. Am.* **1958**, *199*, 31–37.
26. Goldsmid, H.J.; Douglas, R.W. The use of semiconductors in thermoelectric refrigeration. *Br. J. Appl. Phys.* **1954**, *5*, 386.
27. Ioffe, A. *Semiconductor Thermoelements and Thermoelectric Cooling*; Infosearch, Ltd.: London, UK, 1957.
28. Joffe, A. Heat transfer in semiconductors. *Can. J. Phys.* **1956**, *34*, 1342–1355.
29. Joffe, A.F.; Stil'bans, L.S. Physical problems of thermoelectricity. *Rep. Prog. Phys.* **1959**, *22*, 167.
30. Tolman, R.C.; Fine, P.C. On the Irreversible Production of Entropy. *Rev. Mod. Phys.* **1948**, *20*, 51–77.
31. Bridgman, P.W. A Critical Thermodynamic Discussion of the Volta, Thermo-electric and Thermionic Effects. *Phys. Rev.* **1919**, *14*, 306–347.
32. Bridgman, P. On the nature of the transverse thermo-magnetic effect and the transverse thermo-electric effect in crystals. *Proc. Natl. Acad. Sci. USA* **1929**, *15*, 768–773.
33. Bridgman, P. Comments on the Note by E. H. Kennard on "Entropy, Reversible Processes and Thermo-Couples". *Proc. Natl. Acad. Sci. USA* **1932**, *18*, 242–245.
34. Bridgman, P.W. The Second Law of Thermodynamics and Irreversible Processes. *Phys. Rev.* **1940**, *58*, 845.
35. Sommerfeld, A.; Frank, N.H. The Statistical theory of thermoelectric, galvano- and thermomagnetic phenomena in metals. *Rev. Mod. Phys.* **1931**, *3*, 1–42.
36. Darrow, K.K. Statistical Theories of Matter, Radiation and Electricity. *Rev. Mod. Phys.* **1929**, *1*, 90.
37. Haase, R. Thermodynamisch-phänomenologische Theorie der irreversiblen Prozesse. In *Ergebnisse der Exakten Naturwissenschaften*; Springer: Berlin, Germany, 1952; Volume 26, pp. 56–164.
38. Domenicali, C.A. Irreversible Thermodynamics of Thermoelectric Effects in Inhomogeneous, Anisotropic Media. *Phys. Rev.* **1953**, *92*, 877–881.
39. Domenicali, C.A. Irreversible Thermodynamics of Thermoelectricity. *Rev. Mod. Phys.* **1954**, *26*, 237–275.

40. Fieschi, R.; Groot, S.D.; Mazur, P.; Vlieger, J. Thermodynamical theory of galvanomagnetic and thermomagnetic phenomena II: Reciprocal relations for moving anisotropic mixtures. *Physica* **1954**, *20*, 245–258.
41. Fieschi, R.; Groot, S.D.; Mazur, P. Thermodynamical theory of galvanomagnetic and thermomagnetic phenomena. I: Reciprocal relations in anisotropic metals. *Physica* **1954**, *20*, 67–76.
42. Fieschi, R.; Groot, S.D.; Mazur, P. Thermodynamical theory of galvanomagnetic and thermomagnetic phenomena III: Explicit expressions for the measurable effects in isotropic metals. *Physica* **1954**, *20*, 259–273.
43. de Groot, S.; van Kampen, N. On the derivation of reciprocal relations between irreversible processes. *Physica* **1954**, *21*, 39–47.
44. Bernard, W.; Callen, H.B. Irreversible Thermodynamics of Nonlinear Processes and Noise in Driven Systems. *Rev. Mod. Phys.* **1959**, *31*, 1017–1044.
45. Tykodi, R.J. Thermodynamics, Stationary States, and Steady-Rate Processes. III. The Thermocouple Revisited. *J. Chem. Phys.* **1959**, *31*, 1517–1521.
46. Miller, D.G. Thermodynamics of Irreversible Processes. The Experimental Verification of the Onsager Reciprocal Relations. *Chem. Rev.* **1960**, *60*, 15–37.
47. Sherman, B.; Heikes, R.; R.W. Ure, J. Calculation of efficiency of thermoelectric devices. *J. Appl. Phys.* **1960**, *31*, 1–16.
48. Littman, H.; Davidson, B. Theoretical Bound on the Thermoelectric Figure of Merit from Irreversible Thermodynamics. *J. Appl. Phys.* **1961**, *32*, 217–219.
49. Clingman, W. Entropy production and optimum device design. *Adv. Energy Convers.* **1961**, *1*, 61–79.
50. Clingman, W. New Concepts in Thermoelectric Device Design. *Proc. IRE* **1961**, *49*, 1155–1160.
51. Littman, H. A Clarification of the Theoretical Upper Bound on the Thermoelectric “Figure of Merit” Derived from Irreversible Thermodynamics. *J. Appl. Phys.* **1962**, *33*, 2655–2656.
52. El-Saden, M.R. Irreversible Thermodynamics and the Theoretical Bound on the Thermomagnetic Figure of Merit. *J. Appl. Phys.* **1962**, *33*, 3145–3146.
53. Nourbehecht, B. Irreversible thermodynamic effects in inhomogeneous media and their applications in certain geoelectric problems. Technical report for Geophysics Laboratory - Massachusetts Institute of Technology: Cambridge, MA, USA, 1963.
54. Borrego, J. Zener’s maximum efficiency derived from irreversible thermodynamics. *Proc. IEEE* **1964**, *52*, 95.
55. Osterle, J. A unified treatment of the thermodynamics of steady-state energy conversion. *Appl. Sci. Res.* **1964**, *12*, 425–434.
56. Curzon, F.; Ahlborn, B. Efficiency of a Carnot engine at maximum power output. *Am. J. Phys.* **1975**, *43*, 22–24.
57. Andresen, B.; Salamon, P.; Berry, R.S. Thermodynamics in finite time: Extremals for imperfect heat engines. *J. Chem. Phys.* **1977**, *66*, 1571–1577.
58. Hatsopoulos, G.N.; Keenan, J.H., Thermoelectricity. In *Principles of General Thermodynamics*; John Wiley & Sons: New York, NY, USA, 1981; pp. 675–683.

59. Salamon, P.; Nitzan, A. Finite time optimizations of a Newton's law Carnot cycle. *J. Chem. Phys.* **1981**, *74*, 3546–3560.
60. Ondrechen, M.J.; Rubin, M.H.; Band, Y.B. The generalized Carnot cycle: A working fluid operating in finite time between finite heat sources and sinks. *J. Chem. Phys.* **1983**, *78*, 4721–4727.
61. Gupta, V.K.; Shanker, G.; Saraf, B.; Sharma, N.K. Experiment to verify the second law of thermodynamics using a thermoelectric device. *Am. J. Phys.* **1984**, *52*, 625–628.
62. Rockwood, A.L. Relationship of thermoelectricity to electronic entropy. *Phys. Rev. A* **1984**, *30*, 2843–2844.
63. Vos, A.D. Thermodynamics of radiation energy conversion in one and in three physical dimensions. *J. Phys. Chem. Solids* **1988**, *49*, 725 – 730.
64. Mackey, M.C. The dynamic origin of increasing entropy. *Rev. Mod. Phys.* **1989**, *61*, 981.
65. Rowe, D.M., Ed. *CRC Handbook of Thermoelectrics*; RC: Boca Raton, FL, USA, 1995.
66. Rowe, D.M., Ed. *CRC Handbook of Thermoelectrics: Macro to Nano*; RC: Boca Raton, FL, USA, 2006.
67. Snyder, G.J. Thermoelectric Power Generation: Efficiency and Compatibility. In *CRC Handbook of Thermoelectrics: Macro to Nano*; Rowe, D.M., Ed.; Taylor and Francis: Boca Raton, FL, USA, 2006; Chapter 9.
68. Riffat, S.; Ma, X. Thermoelectrics: a review of present and potential applications. *Appl. Therm. Eng.* **2003**, *23*, 913–935.
69. Gordon, J.M. Generalized power versus efficiency characteristics of heat engines: The thermoelectric generator as an instructive illustration. *Am. J. Phys.* **1991**, *59*, 551–555.
70. Lampinen, M.J. Thermodynamic analysis of thermoelectric generator. *J. Appl. Phys.* **1991**, *69*, 4318–4323.
71. Wu, C. Heat transfer effect on the specific power availability of heat engines. *Energy Convers. Manage.* **1993**, *34*, 1239 – 1247.
72. Özkaynak, S.; Gökun, S.; Yavuz, H. Finite-time thermodynamic analysis of a radiative heat engine with internal irreversibility. *J. Phys. D: Appl. Phys.* **1994**, *27*, 1139.
73. Bejan, A. Entropy generation minimization: The new thermodynamics of finite-size devices and finite-time processes. *J. Appl. Phys.* **1996**, *79*, 1191–1218.
74. Bejan, A. Method of entropy generation minimization, or modeling and optimization based on combined heat transfer and thermodynamics. *Revue Gnrale de Thermique* **1996**, *35*, 637 – 646.
75. Parrott, J.E. Thermodynamic Theory of Transport Processes in Semiconductors. *IEEE Trans. Electron Devices* **1996**, *43*, 809–826.
76. Agrawal, D.C.; Menon, V.J. The thermoelectric generator as an endoreversible Carnot engine. *J. Phys. D: Appl. Phys.* **1997**, *30*, 357.
77. Chen, J.; Yan, Z.; Wu, L. Nonequilibrium thermodynamic analysis of a thermoelectric device. *Energy* **1997**, *22*, 979 – 985.
78. Hoffmann, K.H.; Burzler, J.M.; Schubert, S. Endoreversible Thermodynamics. *J. Non-Equilib. Thermodyn.* **1997**, *22*, 311–355.

79. Chen, L.; Wu, C.; Sun, F. Finite Time Thermodynamic Optimization or Entropy Generation Minimization of Energy Systems. *J. Non-Equilib. Thermodyn.* **1999**, *24*, 327–359.
80. Arenas, A.; Vázquez, J.; Sanz-Bobi, M.A.; Palacios, R. Performance of a Thermoelectric Module Using the Thermodynamic Relationship Temperature-Entropy (T-S). In Proceedings of XIX International Conference on Thermoelectrics, Cardiff, UK, 2000.
81. Nuwayhid, R.Y.; Moukalled, F.; Noueihed, N. On entropy generation in thermoelectric devices. *Energy Convers. Manage.* **2000**, *41*, 891–914.
82. Chua, H.T.; Ng, K.C.; Xuan, X.C.; Yap, C.; Gordon, J.M. Temperature-entropy formulation of thermoelectric thermodynamic cycles. *Phys. Rev. E* **2002**, *65*, 056111.
83. Garrido, J. Observable Variables in Thermoelectric Phenomena. *J. Phys. Chem. B* **2002**, *106*, 10722–10724.
84. Xuan, X.C. Optimum design of a thermoelectric device. *Semicond. Sci. Technol.* **2002**, *17*, 114.
85. Bell, L. Alternate thermoelectric thermodynamic cycles with improved power generation efficiencies. In Proceedings of Thermoelectrics, 2003 Twenty-Second International Conference on - ICT, La Grande-Motte, France, 2003.
86. Chakraborty, A. *Thermoelectric cooling devices - thermodynamic modelling and their application in adsorption*. PhD thesis, Department of Mechanical Engineering - National University of Singapore, Singapore, 2005.
87. Chakraborty, A.; Saha, B.; Koyama, S.; Ng, K. Thermodynamic modelling of a solid state thermoelectric cooling device: Temperature-entropy analysis. *Int. J. Heat Mass Transfer* **2006**, *49*, 3547 – 3554.
88. Chakraborty, A.; Ng, K.C. Thermodynamic formulation of temperature-entropy diagram for the transient operation of a pulsed thermoelectric cooler. *Int. J. Heat Mass Transfer* **2006**, *49*, 1845–1850.
89. Pramanick, A.; Das, P. Constructal design of a thermoelectric device. *Int. J. Heat Mass Transfer* **2006**, *49*, 1420–1429.
90. Xuan, X.; Li, D. Thermodynamic analysis of electrokinetic energy conversion. *J. Power Sources* **2006**, *156*, 677–684.
91. Chen, M.; Rosendahl, L.; Bach, I.; Condra, T.; Pedersen, J. Irreversible transfer processes of thermoelectric generators. *Am. J. Phys.* **2007**, *75*, 815–820.
92. Fronczak, A.; Fronczak, P.; Hołyst, J.A. Thermodynamic forces, flows, and Onsager coefficients in complex networks. *Phys. Rev. E* **2007**, *76*, 061106.
93. Izumida, Y.; Okuda, K. Onsager coefficients of a finite-time Carnot cycle. *Phys. Rev. E* **2009**, *80*, 021121.
94. Goddard, J. On the Thermoelectricity of W. Thomson: Towards a Theory of Thermoelastic Conductors. *J. Elast.* **2011**, *104*, 267–280.
95. Vining, C.B. The thermoelectric process. In *Materials Research Society Symposium Proceedings: Thermoelectric Materials - New Directions and Approaches*; Tritt, T., Kanatzidis, M., Lyon, H.B., Jr., Mahan, G., Eds.; Materials Research Society: Warrendale, PA, USA, 1997; pp. 3–13.
96. Strictly speaking, a small interaction level is needed in order to reach thermalization of the gas.

97. The chemical potential is defined as the mean Gibbs free energy per particle. In TE materials, this holds for the electrochemical potential.
98. Normally e is the elementary charge. Here e is negative for electrons, but positive if holes are considered.
99. Agrawal, M. *Basics of Irreversible Thermodynamics*; Stanford University: Stanford, CA, USA, 2008.
100. Tschoegl, N. *Fundamentals of Equilibrium and Steady-state Thermodynamics*; Elsevier Science Ltd: Amsterdam, The Netherlands, 2000.
101. Rocard, Y. *Thermodynamique*, 2nd ed.; Masson: Paris, France, 1967.
102. Prigogine, I. *Introduction to Thermodynamics of Irreversible Processes*, 3rd ed.; John Wiley & Sons, Inc.: New York, NY, USA, 1968.
103. Glansdorff, P.; Prigogine, I. *Thermodynamic Theory of Structure, Stability and Fluctuations*; Wiley-Interscience: New York, NY, USA, 1971.
104. Pottier, N. *Physique statistique hors équilibre, processus irréversibles linéaires*; Savoirs Actuels EDP Sciences/CNRS Editions: Paris, France, 2007.
105. Callen, H.B.; Welton, T.A. Irreversibility and Generalized Noise. *Phys. Rev.* **1951**, *83*, 34–40.
106. Kubo, R. The fluctuation-dissipation theorem. *Rep. Prog. Phys.* **1966**, *29*, 255.
107. Chandler, D. *Introduction to Modern Statistical Mechanics*; Oxford University Press: Oxford, UK, 1987.
108. The off-diagonal terms of the kinetic matrix are symmetric, only if the correct thermodynamic potentials of the system has been chosen. In the case of a Fermi gas the correct potentials are μ_e/T and $1/T$, see Section 2.2 for an example and 5.1 for a counter-example.
109. This time reversal symmetry is broken under the application of Coriolis or magnetic force.
110. Callen, H.B.; Greene, R.F. On a Theorem of Irreversible Thermodynamics. *Phys. Rev.* **1952**, *86*, 702–710.
111. Callen, H.B. *Thermodynamics*; John Wiley & Sons, Inc.: New York, NY, USA, 1960.
112. Zener, C. Putting Electrons to work. *Trans. the Am. Soc. Met.* **1961**, *53*, 1052–1068.
113. The reader will take note of the naming conventions with respect to fluxes and flows: $\dot{Q} = \frac{\partial Q}{\partial t}$ is the **heat transfer rate** or **heat flow** in units of 1 W. For the sake of simplicity the dot is sometimes omitted. Often used is the **heat flux** which is the heat transfer rate per cross-sectional area $J_Q = \frac{1}{A_c} \dot{Q} = \frac{1}{A_c} \frac{\partial Q}{\partial t}$ in units of 1 W/m².
114. With the restriction to one type of semiconductor (p -type, the index can be omitted from the material coefficients in the following calculations, *i.e.*, $\alpha_p = \alpha$ or $K_p = K$).
115. Seifert, W.; Ueltzen, M.; Müller, E. One-dimensional Modelling of Thermoelectric Cooling. *Physica Status Solidi (a)* **2002**, *1*, 277–290.
116. Seifert, W.; Müller, E.; Walczak, S. Generalized analytic description of onedimensional non-homogeneous TE cooler and generator elements based on the compatibility approach. In Proceedings of 25th International Conference on Thermoelectrics, Vienna, Austria, 6–10 August 2006.
117. Harman, T.C.; Honig, J.M. *Thermoelectric and Thermomagnetic Effects and Applications*; McGraw-Hill Book Company: New York, NY, USA, 1967.

118. The Joule effect induced by the circulation of the electrical current has been often considered to be spread over the hot and cold source in equal contributions $\frac{1}{2} R_{in} I^2$. Obviously, this is valid only under CPM condition, see Equations (43), but sufficient for most design.
119. Goldsmid, H.J. *Electronic Refrigeration*; Pion: London, UK, 1986.
120. We follow here Sherman's notation and use φ instead of *C.O.P.* in appropriate formulae.
121. Heikes, R.R.; Roland W. Ure, J. *Thermoelectricity: Science and Engineering*; Interscience Publishers, Inc.: New York, NY, USA, 1961.
122. Egli, P.H. *Thermoelectricity*. John Wiley & Sons, Inc.: New York, NY, USA, 1960.
123. Greene, R.F.; Callen, H.B. On a Theorem of Irreversible Thermodynamics. II. *Phys. Rev.* **1952**, *88*, 1387–1391.
124. Gascoin, F.; Goupil, C.; de Vault, C.; Papavero, A. Non-homogeneous thermoelectric material study using the linear response approach. In Proceedings of The 29th International Conference on Thermoelectrics, Shanghai, China, 30 May–3 June 2010.
125. Ball, C.; Jesser, W.; Maddux, J. The distributed Peltier effect and its influence on cooling devices. In Proceedings of The 14th International Conference on Thermoelectrics, St. Petersburg, Russia, 27–30 June 1995.
126. Buist, R.J. The extrinsic Thomson effect. In Proceedings of The 14th International Conference on Thermoelectrics, St. Petersburg, Russia, 27–30 June 1995.
127. Belov, I.; Volkov, V.; Manyakin, O. Optimization of Peltier thermocouple using distributed Peltier effect. In Proceedings of Eighteenth International Conference on Thermoelectrics, 1999, Piscataway, NJ, USA, 29 August–2 September 1999.
128. Landau, L.D.; Lifshitz, E.M. *Electrodynamics of Continuous Media*, 2nd ed.; Butterworth Heinemann: Oxford, UK, 1984.
129. Snyder, G.J.; Fleurial, J.P.; Caillat, T.; Yang, R.; Chen, G. Supercooling of Peltier cooler using a current pulse. *J. Appl. Phys.* **2002**, *92*, 1564–1569.
130. Stil'bans, L.; Fedorovitch, N. Cooling of thermoelectric cells under nonstationary conditions. *Sov. Phys. Tech. Phys.* **1958**, *3*, 460–463.
131. Parrott, J.E. The interpretation of the stationary and transient behaviour of refrigerating thermocouples. *Solid-State Electron.* **1960**, *1*, 135–143.
132. Gray, P.E. *The Dynamic Behavior of Thermoelectric Devices*; John Wiley & Sons, Inc.: Cambridge, MA, USA, 1960.
133. Reich, A.D.; Madigan, J.R. Transient Response of a Thermocouple Circuit Under Steady Currents. *J. Appl. Phys.* **1961**, *32*, 294–301.
134. Landecker, K.; Findlay, A. Study of the fast transient behaviour of Peltier junctions. *Solid-State Electron.* **1961**, *3*, 239 – 260.
135. Parrott, J. The stationary and transient characteristics of refrigerating thermocouples. *Adv. Energy Convers.* **1962**, *2*, 141–152.
136. Naer, V. Transient regimes of thermoelectric cooling and heating units. *J. Eng. Phys. Thermophys.* **1965**, *8*, 340–344.
137. Iordanishvili, E.K.; Malkovich, B.E.S. Experimental study of transient thermoelectric cooling. *J. Eng. Phys. Thermophys.* **1972**, *23*, 1158–1163.

138. Miner, A.; Majumdar, A.; Ghoshal, U. Thermoelectromechanical refrigeration based on transient thermoelectric effects. *Appl. Phys. Lett.* **1999**, *75*, 1176–1178.
139. Thonhauser, T.; Mahan, G.D.; Zikatanov, L.; Roe, J. Improved supercooling in transient thermoelectrics. *Appl. Phys. Lett.* **2004**, *85*, 3247–3249.
140. Bechtold, T.; Rudnyi, E.B.; Korvink, J.G. Dynamic electro-thermal simulation of microsystems - a review. *J. Micromech. Microeng.* **2005**, *15*, R17–R31.
141. Hussein, M.; Hanim, S.; Zamri, Y.M. The transient response for different types of erodable surface thermocouples using finite element analysis. *Therm. Sci.* **2007**, *11*, 49–64.
142. Zhou, Q.; Bian, Z.; Shakouri, A. Pulsed cooling of inhomogeneous thermoelectric materials. *J. Phys. D: Appl. Phys.* **2007**, *40*, 4376–4381.
143. Ursell, T.; Snyder, G. Compatibility of segmented thermoelectric generators. In Proceedings of Twenty-First International Conference on Thermoelectrics, Long Beach, CA, USA, 25 August–29 August 2002.
144. Snyder, G.J.; Ursell, T.S. Thermoelectric Efficiency and Compatibility. *Phys. Rev. Lett.* **2003**, *91*, 148301.
145. A more general definition of u seems possible when writing the relative current density in terms of fluctuating currents which are indeed 3D. In this context, particle and heat flow should be considered in an anisotropic medium where the material parameters are tensors, see e.g., [174].
146. Goupil, C. Thermodynamics of the thermoelectric potential. *J. Appl. Phys.* **2009**, *106*, 104907.
147. Power output is defined here according to thermodynamic rules: quantities input to the system are positive.
148. Seifert, W.; Zabrocki, K.; Müller, E.; Snyder, G. Power-related compatibility and maximum electrical power output of a thermogenerator. *Phys. Stat. Sol. A* **2010**, *207*, 2399–2406.
149. The Carnot engine exchanges energy in a reversible form, that means after an infinite time. Therefore, the Carnot engine transforms energy efficiently but with zero power.
150. Replace in [116] Equation (9), right hand side, the \pm sign by a minus sign valid for both the pump up and the pump down situation.
151. Seifert, W.; Müller, E.; Snyder, G.; Walczak, S. Compatibility factor for the power output of a thermogenerator. *Phys. Stat. Sol. (RRL)* **2007**, *1*, 250–252.
152. Seifert, W.; Müller, E.; Walczak, S. Local optimization strategy based on first principles of thermoelectrics. *Phys. Stat. Sol. A* **2008**, *205*, 2908–2918.
153. Seifert, W.; Zabrocki, K.; Snyder, G.; Müller, E. The compatibility approach in the classical theory of thermoelectricity seen from the perspective of variational calculus. *Phys. Stat. Sol. A* **2010**, *207*, 760–765.
154. In [116] and [153] reduced efficiencies $\eta_r^{(g)} \equiv \eta_r$, $\eta_r^{(c)} \equiv \varphi_r$ are introduced for both TEG and TEC, respectively.
155. Seifert, W.; Pluschke, V.; Goupil, C.; Zabrocki, K.; Müller, E.; Snyder, G. Maximum performance in self-compatible thermoelectric elements. *J. Mater. Res.* **2011**, in press.

156. The relative current density is defined by Equation (75); the 1D variants are $u(x) = -\frac{J}{\kappa T'(x)}$ respectively $u(T) = -\frac{J}{\kappa}x'(T)$, whereby the temperature gradient decides the sign of u . Note that $T(x)$ peaks in the interior of the TE element only far above the optimum current for maximum efficiency and maximum coefficient of performance. Then u has a pole.
157. Note that Sherman et al. used the function $\epsilon(T)$ instead of optimal reduced efficiency.
158. Cadoff, I.B.; Miller, E. The thermoelectric circuit. In *Thermoelectric Materials and Devices*; Cadoff, I.B., Miller, E., Eds.; Materials Technology Series. Reinhold Publishing Cooperation: New York, NY, USA, 1960; Chapter 2, pp. 18–32.
159. Kerr, D.L. Design calculations for thermoelectric generators. In *Thermoelectric Materials and Devices*; Cadoff, I.B., Miller, E., Eds.; Materials Technology Series. Reinhold Publishing Cooperation: New York, NY, USA, 1960; Chapter 16, pp. 227–249.
160. Vought, R.H. Design calculations for Peltier cooling. In *Thermoelectric Materials and Devices*; Cadoff, I.B., Miller, E., Eds., Materials Technology Series. Reinhold Publishing Cooperation: New York, 1960, chapter 17, pp. 250–274.
161. Sickert, R. A Thermoelectric Refrigerating System for Submarines. *Electr. Eng.* **1960**, *79*, 364–371.
162. Ure, Jr., R.W.; Heikes, R.R., Theoretical Calculation of Device Performance. In *Thermoelectricity: Science and Engineering*; Heikes, R.R., Ure, R.W., Jr., Eds.; Interscience Publishers, Inc.: New York, NY, USA, 1961; Chapter 15, pp. 458–517.
163. Min, G.; Rowe, D.M. Peltier Devices as Generators. In *CRC Handbook of Thermoelectrics*; Rowe, D.M., Ed.; CRC Press: RC, Boca Raton, FL, USA, 1995; Chapter 38, pp. 479–488.
164. Min, G. Thermoelectric Module Design Theories. In *CRC Handbook of Thermoelectrics: Macro to Nano*; Rowe, D.M., Ed.; Taylor and Francis: Boca Raton, FL, USA, 2006; Chapter 11.
165. Shiota, I.; Miyamoto, Y., Eds. *Functionally Graded Material 1996*; AIST Tsukuba Research Center: Tsukuba, Japan, 1996.
166. Helmers, L.; Müller, E.; Schilz, J.; Kaysser, W. Graded and stacked thermoelectric generators - numerical description and maximisation of output power. *Mater. Sci. Eng., B* **1998**, *56*, 60–68.
167. Müller, E.; Drašar, Č.; Schilz, J.; Kaysser, W.A. Functionally graded materials for sensor and energy applications. *Mater. Sci. Eng. A* **2003**, *362*, 17–39.
168. Kuznetsov, V.L. Functionally Graded Materials for Thermoelectric Applications. In *CRC Handbook of Thermoelectrics: Macro to Nano*; Taylor and Francis: Boca Raton, FL, USA, 2006; Chapter 38.
169. Müller, E.; Zabrocki, K.; Goupil, C.; Snyder, G.; Seifert, W. Functionally graded thermoelectric generator and cooler elements. In *CRC Handbook of Thermoelectrics: Thermoelectrics and Its Energy Harvesting*; Rowe, D.M., Ed.; RC: Boca Raton, FL, USA, 2012; Chapter 4.
170. Zabrocki, K.; Müller, E.; Seifert, W.; Trimper, S. Performance optimization of a thermoelectric generator element with linear material profiles in a 1D setup. *J. Mater. Res.* **2011**, in press.
171. Müller, E.; Walczak, S.; Seifert, W. Optimization strategies for segmented Peltier coolers. *Phys. Stat. Sol. A* **2006**, *203*, 2128–2141.
172. Anatyshuk, L. Seebeck or Volta? *J. Thermoelectricity* **1994**, *1994*, 9–10.

173. Anatyчук, L. On the discovery of thermoelectricity by Volta. *J. Thermoelectricity* **2004**, *2004*, 5–10.
174. Buda, I.S.; Lutsyak, V.S.; Khamets, U.M.; Shcherbina, L.A. Thermodynamic definition of the thermoelectric figure of merit of an anisotropic medium. *Phys. Stat. Sol. A* **1991**, *123*, K139–K143.

© 2011 by the authors; licensee MDPI, Basel, Switzerland. This article is an open access article distributed under the terms and conditions of the Creative Commons Attribution license (<http://creativecommons.org/licenses/by/3.0/>.)